[redacted]

Copy 75
RM H55D12

NACA RM H55D12

LIBRARY NACA - HSFS

RESEARCH MEMORANDUM

FLIGHT MEASUREMENTS OF WING LOADS ON THE CONVAIR XF-92A DELTA-WING AIRPLANE

By Albert E. Kuhl and Clinton T. Johnson

High-Speed Flight Station
Edwards, Calif.

CLASSIFICATION CHANGED
TO unclassified
BY AUTHORITY OF Decl Ba 111 DATE

LIBRARY NACA - HSFS

CLASSIFIED DOCUMENT

This material contains information affecting the National Defense of the United States within the meaning of the espionage laws, Title 18, U.S.C., Secs. 793 and 794, the transmission or revelation of which in any manner to an unauthorized person is prohibited by law.

NATIONAL ADVISORY COMMITTEE FOR AERONAUTICS

WASHINGTON

May 25, 1955

[redacted]

LIBRARY NACA - HSFS

NATIONAL ADVISORY COMMITTEE FOR AERONAUTICS

RESEARCH MEMORANDUM

FLIGHT MEASUREMENTS OF WING LOADS ON THE CONVAIR XF-92A DELTA-WING AIRPLANE

By Albert E. Kuhl and Clinton T. Johnson

SUMMARY

A flight investigation was made at altitudes from 30,000 feet to 35,000 feet to determine the wing loads on the Convair XF-92A airplane over the lift range of the airplane at subsonic and transonic speeds. The theoretical lift-curve slope for a delta wing was calculated and compared with the flight data at a Mach number of 0.75.

The wing-panel characteristics display nonlinearities with increasing angle of attack. The wing-panel bending-moment coefficient has nonlinear characteristics throughout the angle-of-attack range, whereas the wing-panel normal-force and pitching-moment coefficients become nonlinear at the higher angles of attack.

In the low-lift region, below the decrease in longitudinal stability, the wing-panel normal-force and pitching-moment coefficients due to angle of attack increase approximately 20 percent of the low-speed values up to a Mach number of 0.83 where the wing reaches its critical Mach number. Above the wing critical Mach number, abrupt changes take place in both parameters with indications of returning to the level of the low-speed values at the highest Mach numbers tested. The lateral center of pressure is located from about 42 percent to 45 percent of the wing-panel semispan for the Mach number range of these tests.

The wing-panel normal-force, pitching-moment, and bending-moment coefficients due to elevon deflection, determined in the low-lift region, decrease with increasing Mach number above a Mach number near 0.75.

INTRODUCTION

As part of the cooperative Air Force—Navy—NACA flight research program the National Advisory Committee for Aeronautics utilized the Convair XF-92A delta-wing airplane for flight investigations at the NACA High-Speed Flight Station at Edwards, Calif.

LIBRARY NACA - HSFS

The primary purpose of these flight investigations was to evaluate the handling qualities, lift and drag characteristics, aerodynamic loads and load distribution, control surface loads, and buffeting characteristics. During the test program the flight envelope of the airplane was extended to maximum lift and Mach number attainable. Stability considerations necessitated the performance of these tests at high altitudes.

This paper presents the results of the measured aerodynamic loads on the wing during wind-up turn maneuvers covering the Mach number range from stall to transonic speeds.

SYMBOLS

BM_W left wing-panel bending moment about wing-panel strain-gage station, in-lb

$b_W/2$ span of left wing panel outboard of gage station, in.

C_{B_W} wing-panel bending-moment coefficient, $\dfrac{BM_W}{q\,\frac{S_W}{2}\,\frac{b_W}{2}}$

C_{B_δ}' variation of wing-panel bending-moment coefficient with elevon deflection, per degree, $\partial C_{B_W}/\partial \delta_{e_L}$

$\left(C_{B_W}\right)_{\delta_{e_L}=0}$ wing-panel bending-moment coefficient corrected to zero elevon deflection, $C_{B_W} - \left(C_{B_\delta}' \times \delta_{e_L}\right)$

$C_{m_{\bar{c}_W/4}}$ wing-panel pitching-moment coefficient about quarter chord of wing-panel mean aerodynamic chord, $\dfrac{M_W}{q\,\frac{S_W}{2}\,\bar{c}_W}$

C_{m_α}' variation of wing-panel pitching-moment coefficient with angle of attack at zero elevon deflection, per degree, $\dfrac{\partial C_{m_{\bar{c}_W/4}}}{\partial \alpha}$

C_{m_δ}' variation of wing-panel pitching-moment coefficient with elevon deflection, per degree, $\dfrac{\partial C_{m_{\bar{c}_W/4}}}{\partial \delta_{e_L}}$

$\left(C_{m_{\bar{c}_W/4}}\right)_{\delta_{e_L}=0}$ wing-panel pitching-moment coefficient corrected to zero elevon deflection, $C_{m_{\bar{c}_W/4}} - \left(C_{m_\delta}' \times \delta_{e_L}\right)$

C_{N_A} airplane normal-force coefficient, $\frac{nW}{qS}$

C_{N_W} left wing-panel normal-force coefficient, $\frac{L_W}{q\,\frac{S_W}{2}}$

C_{N_α}' variation of wing-panel normal-force coefficient with angle of attack at zero elevon deflection, per degree, $\frac{\partial C_{N_W}}{\partial \alpha}$

C_{N_δ}' variation of wing-panel normal-force coefficient with elevon deflection, per degree, $\frac{\partial C_{N_W}}{\partial \delta_{e_L}}$

$\left(C_{N_W}\right)_{\delta_{e_L}=0}$ wing-panel normal-force coefficient corrected to zero elevon deflection, $C_{N_W} - \left(C_{N_\delta}' \times \delta_{e_L}\right)$

c_W chord at any section, ft

$\bar{c}_W$ mean aerodynamic chord of the wing panel, 174.4 in.,

$$\frac{\int_0^{b_W/2} c_W^2 dy}{\int_0^{b_W/2} c_W dy}$$

g acceleration due to gravity, ft/sec^2

L_W left wing-panel aerodynamic load, lb

M free-stream Mach number

M_W left wing-panel pitching moment about the quarter chord of wing-panel mean aerodynamic chord, in-lb

n	normal-load factor, g units
q	free-stream dynamic pressure, lb/sq ft
S	total wing area, including area projected through fuselage, 425.0 sq ft
$S_W/2$	area of left wing panel outboard of strain-gage station, 137.1 sq ft
t	time, sec
W	airplane gross weight, lb
y	distance along span, in.
y_{cp}	wing-panel lateral center-of-pressure location at zero elevon deflection, percent of $b_W/2$
α_i	indicated angle of attack, deg
δ_{e_L}	left elevon position, deg
$\dot{\theta}$	pitching velocity, radians/sec
$\ddot{\theta}$	pitching acceleration, radians/sec^2

AIRPLANE

The Convair XF-92A is a semitailless delta-wing airplane having a 60° sweepback at the leading edge of the wing and vertical stabilizer. The wing-elevon combination and the vertical tail have a streamwise thickness ratio of 6.5 percent. The elevons and rudder are full-span constant-chord surfaces with small unshielded horn balances near the tips. Control surfaces are actuated by a 100-percent hydraulically boosted system. The airplane has no dive brakes and no leading- or trailing-edge flaps or slats.

A three-view drawing of the airplane is shown in figure 1 and photographs are shown in figure 2. Table I lists the physical characteristics of the airplane.

INSTRUMENTATION AND ACCURACY

The XF-92A airplane was equipped with standard NACA recording instruments for recording the following quantities pertinent to this investigation:

Airspeed
Altitude
Normal, longitudinal, and transverse accelerations
Pitching angular velocity and acceleration
Rolling angular velocity and acceleration
Control positions
Angle of attack and angle of sideslip

A multichannel oscillograph was used for recording strain-gage outputs. All instruments were correlated by a common timer.

Strain gages were installed on the wing spars and skin at the wing root (approximately 4 inches outboard of the wing fuselage juncture as shown in fig. 1) to measure shear, bending moment, and torque. The data presented in this paper have been corrected for the inertia of the wing and are therefore the aerodynamic loads acting over the wing panel. Based on the results of the static calibration and an evaluation of the strain-gage responses in flight, the estimated accuracies of the measured shear, bending moment, and torque are ±300 pounds, ±7,000 inch-pounds, and ±25,000 inch-pounds, respectively.

Indicated angle of attack was measured by a vane located on the nose boom and was corrected only for deflections of the boom. The estimated accuracy of the angle-of-attack recorder is ±0.5°. Accuracies of other pertinent recorded quantities are:

Mach number, M	±0.01
Normal acceleration, n, g units	±0.05
Elevon position, δ_{e_L}, deg	±0.20
Pitching velocity, $\dot{\theta}$, radians/sec	±0.02
Pitching acceleration, $\ddot{\theta}$, radians/sec^2	±0.05

TESTS

The tests were conducted in a clean configuration with no wing fences installed on the airplane. The tests consisted of longitudinal elevon pulses and wind-up turns over the Mach number range from 0.43 to 0.95 at altitudes from 30,000 feet to 35,000 feet. Reynolds number,

based on the wing mean aerodynamic chord, varied between 21.7×10^6 and 48.9×10^6 for these tests. The center of gravity of the airplane varied between 27.2 and 28.7 percent of wing mean aerodynamic chord.

PROCEDURE

The wing-panel normal-force, pitching-moment, and bending-moment coefficients due to elevon deflection C_{N_δ}', C_{m_δ}', and C_{B_δ}' were determined from abrupt elevon deflection maneuvers. The wing-panel coefficients were determined from the portion of the pulse where the surface deflection reached approximately maximum value and the airplane response to the control input was minimum. All measurements were taken before the angle of attack had changed more than $1/4^\circ$. A change of angle of attack of this magnitude would cause estimated errors of about 30 percent in C_{N_δ}' and 20 percent in C_{m_δ}' based on the values of wing-panel normal-force coefficient and pitching-moment coefficient due to angle of attack C_{N_α}' and C_{m_α}' determined from this investigation. The error in C_{B_δ}' was estimated to be approximately 30 percent.

The parameters C_{N_α}' and C_{m_α}' were derived from wind-up turn maneuvers by subtracting the normal-force and pitching-moment coefficients due to elevon deflection from the measured data obtained during the maneuvers. The resultant normal-force and pitching-moment coefficients, corrected to a condition of zero elevon deflection, were plotted against angle of attack and least-squares slopes were calculated to yield C_{N_α}' and C_{m_α}'.

The wing-panel lateral center of pressure for zero elevon deflection y_{cp} was determined by dividing the wing-panel bending-moment coefficient $\left(C_{B_W}\right)_{\delta_{e_L}=0}$ by the wing-panel normal-force coefficient $\left(C_{N_W}\right)_{\delta_{e_L}=0}$.

RESULTS AND DISCUSSION

Data from longitudinal elevon pulses are shown in figure 3 as the variation with time of left elevon position, wing-panel normal-force, bending-moment, and pitching-moment coefficients, pitching velocity,

and angle of attack. From these maneuvers the wing-panel coefficients due to elevon deflection C_{N_δ}', C_{m_δ}', and C_{B_δ}' were determined by dividing the measured incremental values of wing-panel normal-force coefficient, wing-panel pitching-moment coefficient, and wing-panel bending-moment coefficient by the corresponding elevon deflection. The portions of the maneuver used in determining C_{N_δ}', C_{m_δ}', and C_{B_δ}' are indicated by the solid lines on figure 3. Only this initial portion of the maneuver was used in order to reduce errors caused by a change in angle of attack.

The parameters C_{N_δ}', C_{m_δ}', and C_{B_δ}' (fig. 4) remain constant with increasing Mach number up to a Mach number of approximately 0.75, then decrease as higher Mach numbers are reached. The parameter C_{N_δ}' changes from a level of 0.024, over the lower Mach number range, to a value of 0.005 at a Mach number of 0.95, while C_{m_δ}' and C_{B_δ}' change from levels of -0.01 and 0.01 at the lower Mach numbers to values of -0.005 and 0.005, respectively, at a Mach number of 0.95.

Data from wind-up turns at representative Mach numbers are shown in figure 5 as the variation with time of Mach number, angular pitching acceleration, wing-panel pitching-moment, bending-moment, and normal-force coefficients, airplane normal-force coefficient, left elevon position, and angle of attack. The XF-92A airplane experiences a reduction in longitudinal stability at the higher angles of attack (ref. 1). The angle of attack at which the reduction occurs is shown in the figures by the vertical line above the curves. During the low-speed turn shown in figure 5(a) a reduction in longitudinal stability was not apparent and no vertical line is shown above the angle-of-attack curve. Above the angle of attack of the reduction in longitudinal stability the airplane experiences relatively large pitching accelerations.

Figure 6 shows the data of figure 5 as a function of angle of attack. The angle of attack at which the airplane experienced a reduction in longitudinal stability is again indicated by the vertical lines above these curves. Nonlinear variations with angle of attack are apparent in the wing-panel characteristics particularly at the higher angles of attack above the reduction in stability. Nonlinear variations are also evident in the airplane normal-force-coefficient and elevon-position curves.

To remove the effects of elevon deflection and evaluate the effect of angle of attack on the wing-panel normal-force- and pitching-moment-coefficient curves, the data of figure 6 were corrected to a condition of zero elevon deflection by using the previously determined values of C_{N_δ}' and C_{m_δ}'. The variation of the wing-panel normal-force and pitching-moment coefficients, corrected to zero elevon deflection, with

angle of attack is shown in figure 7 with the angle of attack of the airplane stability boundary again indicated by the vertical line above the curves. These curves are essentially linear up to the angle of attack of the reduction in airplane stability and become nonlinear thereafter with irregular characteristics occurring near the pitch-up. The region above the reduction in airplane stability is characterized by large angular pitching and rolling accelerations. Therefore, it is assumed that the corrections applied to the data above the stability boundary are not valid since they were obtained by using values of C_{N_δ}' and C_{m_δ}' measured in the low-lift region. However, the corrected data indicate that at the higher angles of attack abrupt changes occur in the normal-force-coefficient data caused by either C_{N_δ}' or C_{N_α}', with similar changes occurring in the pitching-moment-coefficient data caused by either C_{m_δ}' or C_{m_α}'. Trends similar to those of the corrected data in the upper lift region have been reported in reference 2 from wind-tunnel tests at zero elevon deflection of a 6-percent-thick delta-wing having 60° leading-edge sweepback. In determining values of C_{N_α}' and C_{m_α}' only the data below the airplane stability boundary, where the data are essentially linear, were considered. The values of C_{N_α}' and C_{m_α}' for the low-lift region were determined by taking least-squares slopes of the data in figure 7. The slopes obtained by this method are shown on the curves. The values of C_{N_α}' and C_{m_α}' obtained for the low-lift region from the slopes drawn in figure 7 are presented in figure 8 as the variation of C_{N_α}' and C_{m_α}' with Mach number.

The parameter C_{N_α}' increases gradually from a value of about 0.045 at a Mach number of 0.47 to a value of about 0.053 at a Mach number of 0.83, followed by a rather abrupt increase to a peak value of about 0.062 at a Mach number of 0.88. Thereafter C_{N_α}' abruptly decreases to about its low-speed value at a Mach number near 0.91.

The theoretical value of the lift-curve slope of the wing panel in the presence of the fuselage at a Mach number of 0.75 was calculated by the method of reference 3 and is shown in figure 8. The results indicate good agreement between the theoretical and the flight values.

The parameter C_{m_α}' (fig. 8) shows a similar variation, increasing gradually from a value of -0.007 at a Mach number of 0.47 to a value of -0.0085 at a Mach number of 0.83. A more abrupt increase in C_{m_α}' then takes place reaching a peak value of about -0.0125 at a Mach number

LIBRARY NACA - HSFS

of 0.88. Thereafter C_{m_α}' decreases to a value of about -0.010 at a Mach number of 0.91. The abrupt changes in the parameters C_{N_α}' and C_{m_α}' near a Mach number of 0.83 occur near the wing critical speed (ref. 4).

Figure 9 shows the variation of wing-panel bending-moment coefficient and lateral center of pressure with wing-panel normal-force coefficient for zero elevon deflection at representative Mach numbers. The point of reduction of airplane stability is indicated by the vertical line above each of these curves. All the bending-moment-coefficient curves display a similar trend, a general rounding over throughout the lift range, which becomes more pronounced at normal-force coefficients above the reduction in airplane stability.

The general rounding over of the bending-moment curves is reflected as a gradual inboard movement of the lateral center of pressure with increasing lift. At low and moderate lifts the center of pressure is located from about 42-percent to 45-percent wing-panel semispan over the Mach number range of these tests.

CONCLUSIONS

Flight measurements of the wing loads on the Convair XF-92A airplane over the Mach number range from 0.43 to 0.95 have indicated the following:

1. The wing-panel characteristics generally display nonlinearities with increasing angle of attack. The wing-panel bending-moment coefficient has nonlinear characteristics throughout the angle-of-attack range, whereas the wing-panel normal-force and pitching-moment coefficients become nonlinear at the higher angles of attack.

2. The wing-panel normal-force and pitching-moment coefficients due to angle of attack increase approximately 20 percent of their low-speed values up to a Mach number of 0.83 where the wing reaches its critical Mach number. Above this Mach number abrupt changes take place in both parameters with indications of returning to a level near their low-speed values at the highest Mach numbers tested. The lateral center of pressure is located from about 42 percent to 45 percent of the wing-panel semispan for the Mach number range of these tests.

LIBRARY NACA - HSFS

3. The wing-panel normal-force, pitching-moment, and bending-moment coefficients due to elevon deflection, determined in the low-lift region, decrease with increasing Mach number above a Mach number near 0.75.

High-Speed Flight Station,
National Advisory Committee for Aeronautics,
Edwards, Calif., March 23, 1955.

REFERENCES

1. Sisk, Thomas R., and Muhleman, Duane O.: Longitudinal Stability Characteristics in Maneuvering Flight of the Convair XF-92A Delta-Wing Airplane Including the Effects of Wing Fences. NACA RM H54J27, 1955.

2. Palmer, William E.: Effect of Reduction in Thickness From 6 to 2 Percent and Removal of the Pointed Tips on the Subsonic Static Longitudinal Stability Characteristics of a 60° Triangular Wing in Combination With a Fuselage. NACA RM L53F24, 1953.

3. Zlotnick, Martin, and Diederich, Franklin W.: Theoretical Calculation of the Effect of the Fuselage on the Spanwise Lift Distribution on a Wing. NACA RM L51J19, 1952.

4. Keener, Earl R.: Wing Pressure Distributions at Low Lift for the XF-92A Delta-Wing Airplane at Transonic Speeds. NACA RM H54H06, 1954.

TABLE I

PHYSICAL CHARACTERISTICS OF THE XF-92A AIRPLANE

Wing:	
Area, sq ft	425
Span, ft	31.33
Airfoil section	NACA $65_{(06)}$-006.5
Mean aerodynamic chord, ft	18.09
Aspect ratio	2.31
Root chord, ft	27.13
Tip chord	0
Taper ratio	0
Sweepback (leading edge), deg	60
Incidence, deg	0
Dihedral (chord plane), deg	0
Wing panel:	
Area, sq ft	137.1
Span, in.	150.9
Mean aerodynamic chord, in.	174.4
Fuselage station of leading edge of mean aerodynamic chord, in.	274.29
Elevons:	
Area (total of both elevons rearward of hinge line), sq ft	76.19
Horn-balance area (total of both elevons forward of hinge line), sq ft	1.4
Span (one elevon), ft	13.35
Chord (rearward of hinge line, constant except at tip), ft	3.05
Movement, deg	
Elevator:	
Up	15
Down	5
Aileron, total	10
Operation	Hydraulic
Vertical tail:	
Area, sq ft (exposed)	75.35
Height, above fuselage center line, ft	11.50
Airfoil section	NACA $65_{(06)}$-006.5
Mean aerodynamic chord, in.	167.5
Aspect ratio	2.31
Root chord, in.	251.2
Tip chord	0
Taper ratio	0
Sweepback (leading edge), deg	60
Rudder:	
Area, sq ft	15.53
Span, ft	9.22
Travel, deg	±8.5
Operation	Hydraulic
Fuselage:	
Length, ft	42.80
Maximum diameter, ft	5.58
Power plant:	
Engine	Allison J33-A-29 with afterburner
Rating:	
Static thrust at sea level, lb	5,600
Static thrust at sea level with afterburner, lb	7,500
Weight:	
Gross weight (560 gal fuel), lb	15,560
Empty weight, lb	11,808
Center-of-gravity locations:	
Gross weight (560 gal fuel), percent M.A.C.	25.5
Empty weight, percent M.A.C.	29.2
Moment of inertia in pitch, slug-ft^2	35,000

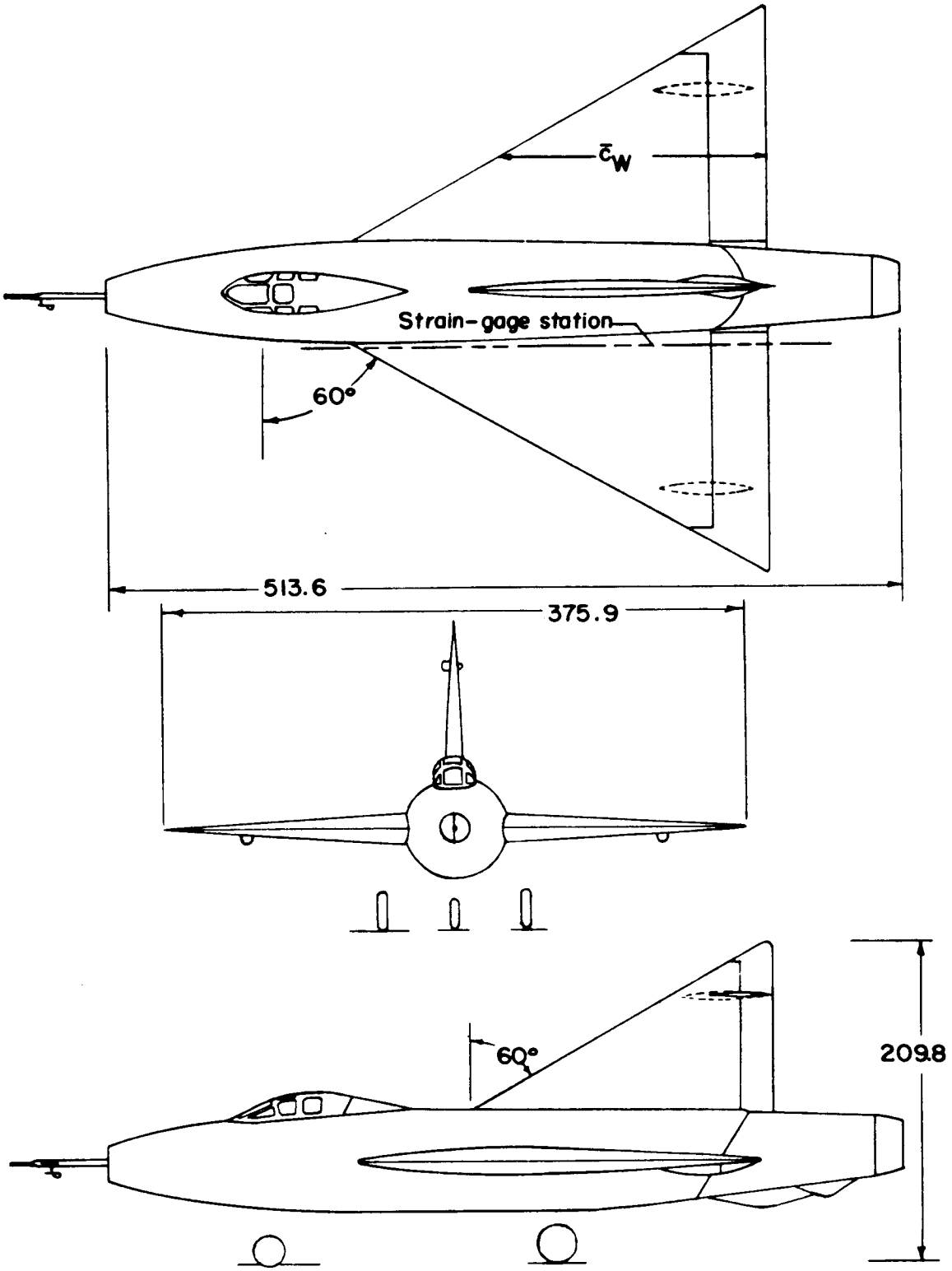

Figure 1.- A three-view drawing of the XF-92A airplane. All dimensions in inches.

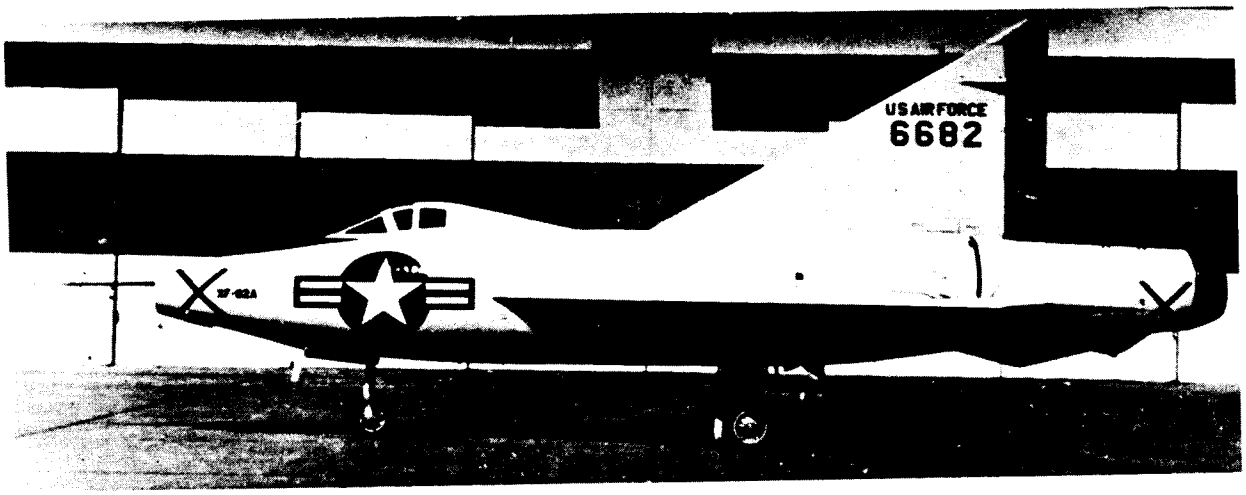

(a) Left side view.

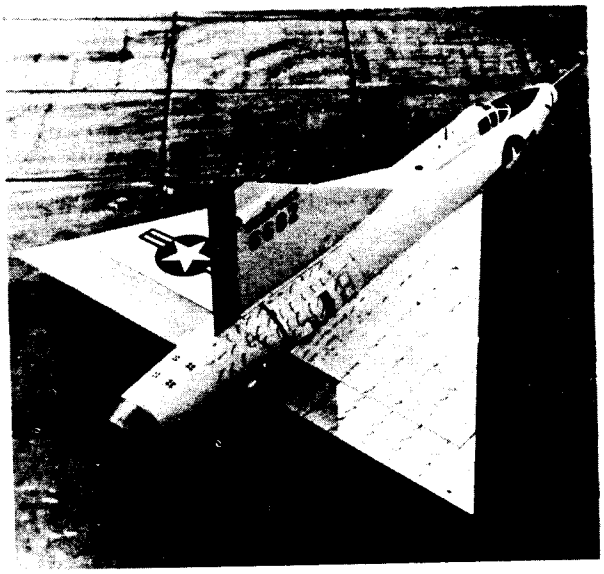

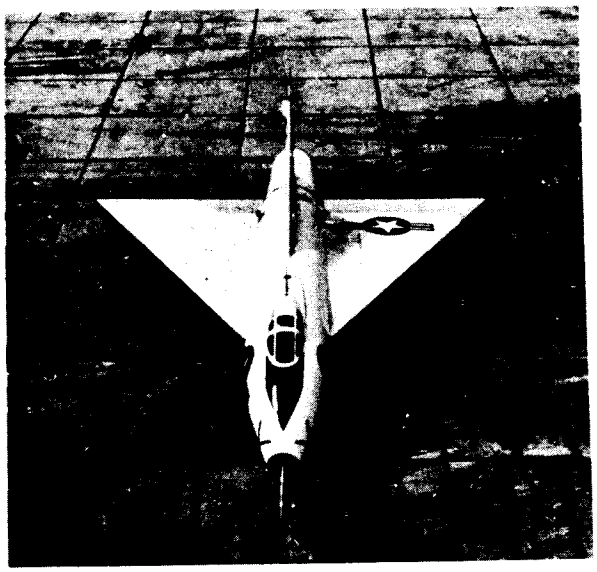

L-87923

(b) Three-quarter rear view. (c) Overhead front view.

Figure 2.- Photographs of XF-92A research airplane.

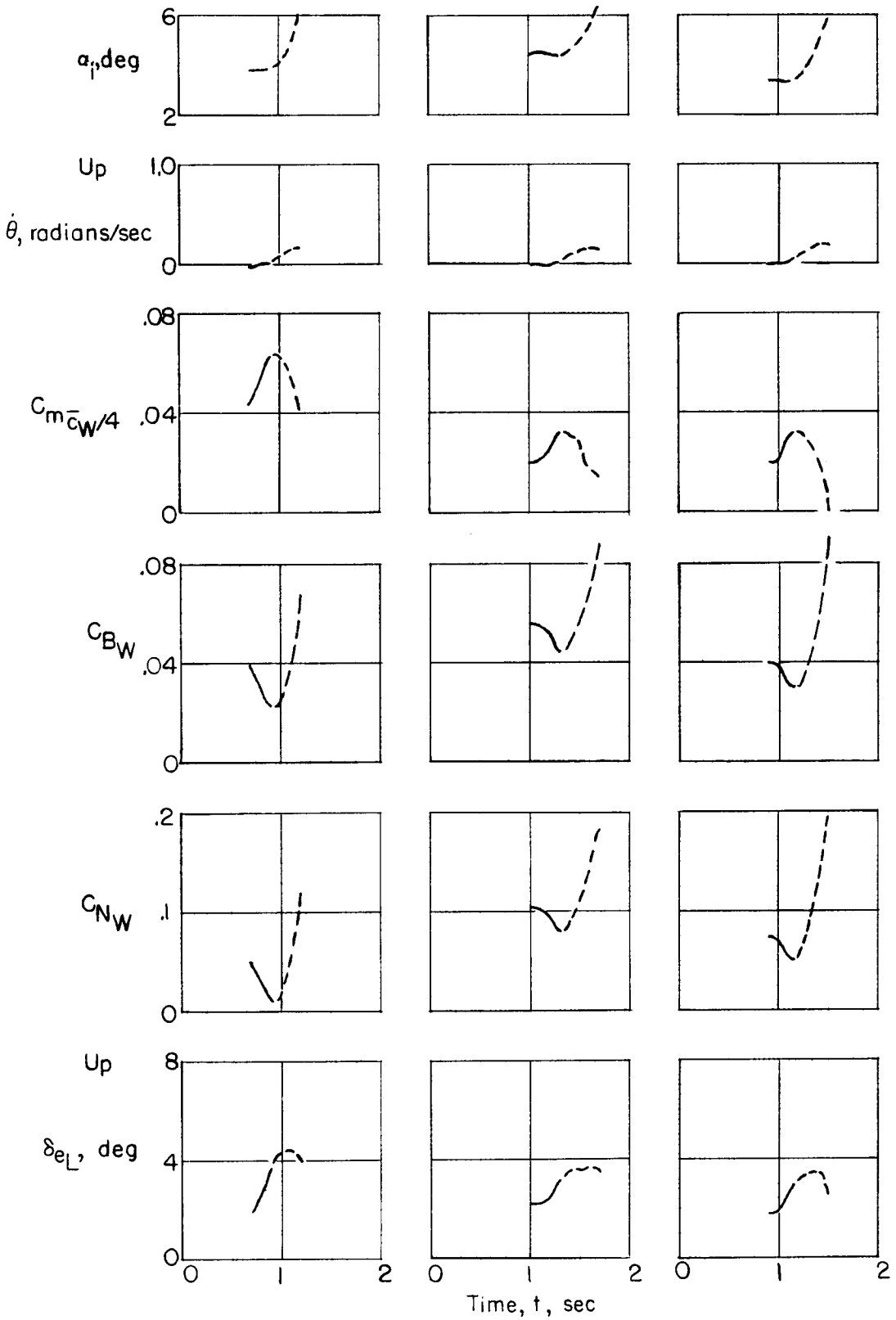

(a) M ≈ 0.59. (b) M ≈ 0.69. (c) M ≈ 0.77.

Figure 3.- Time histories of longitudinal elevon pulses.

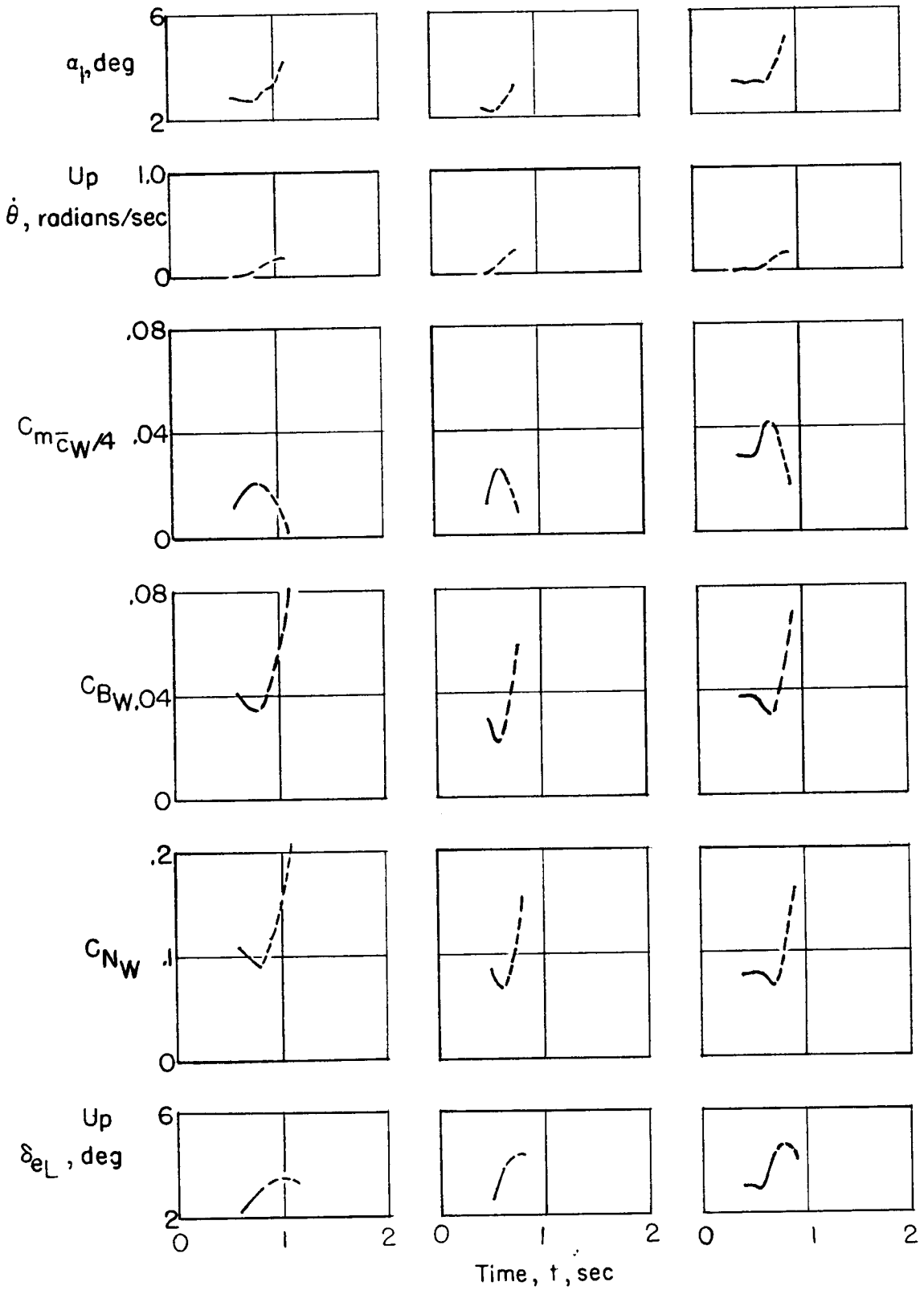

(d) M ≈ 0.84. (e) M ≈ 0.90. (f) M ≈ 0.92.

Figure 3.- Concluded.

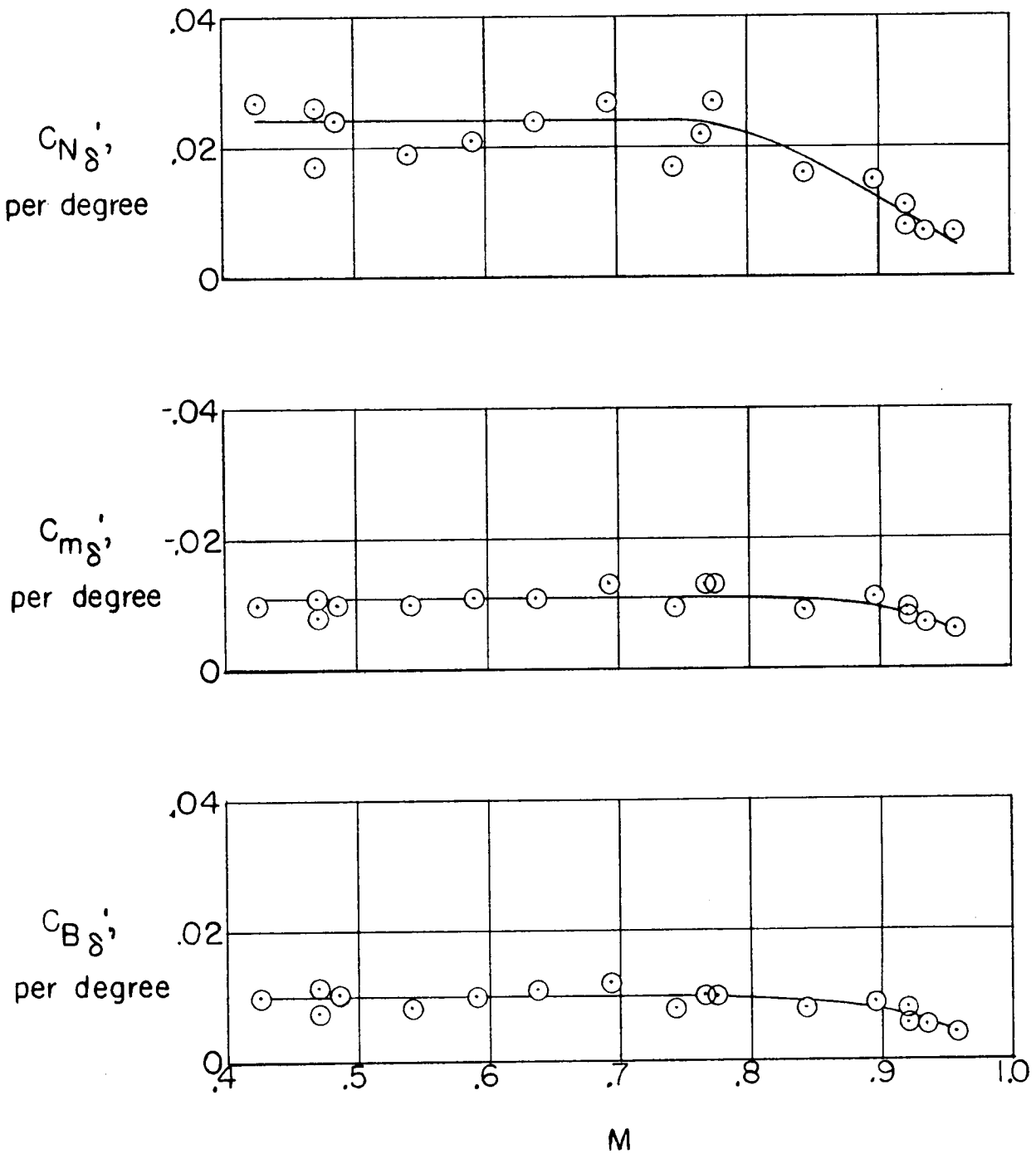

Figure 4.- Variation of normal-force, pitching-moment, and bending-moment coefficients due to elevon deflection with Mach number.

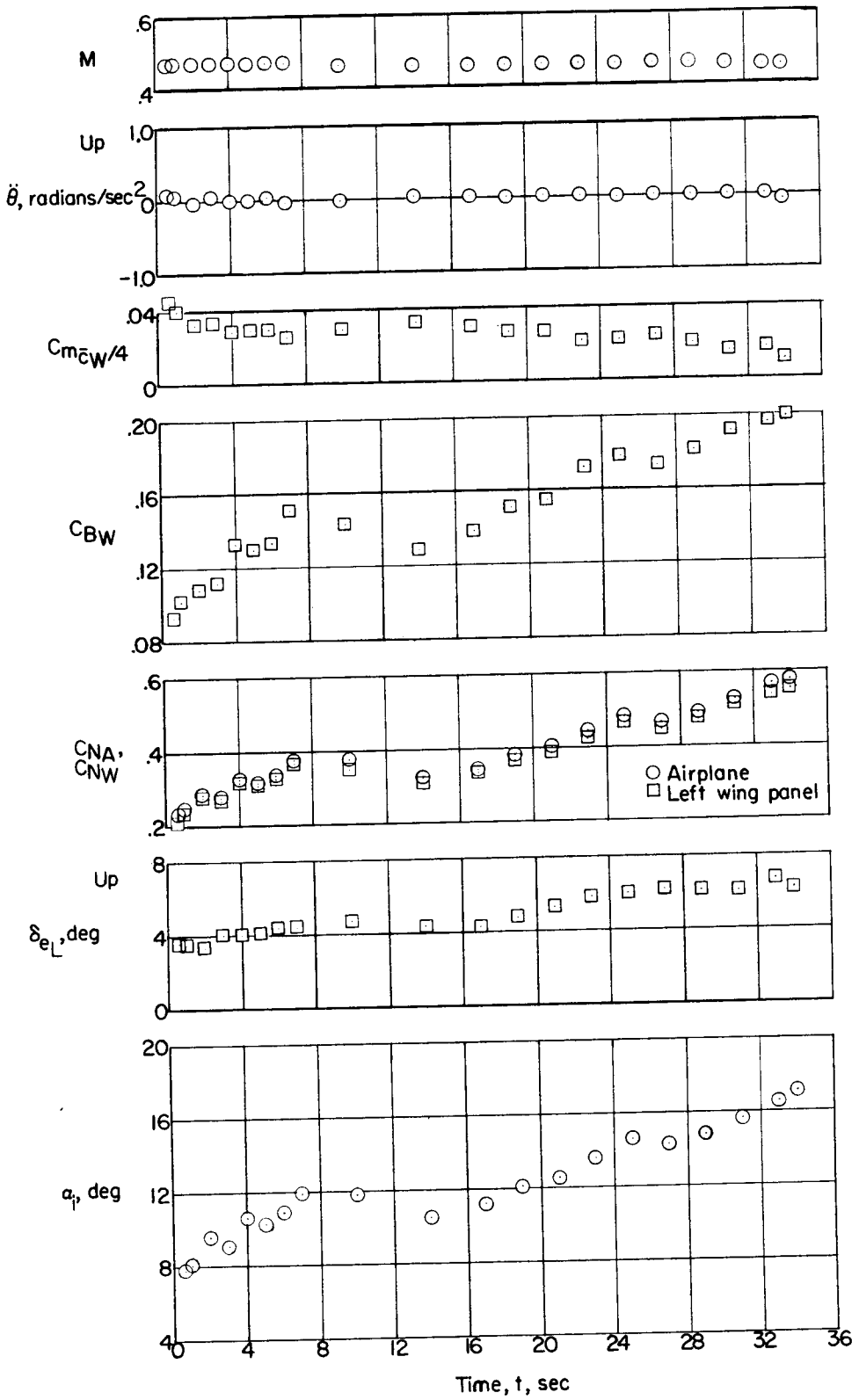

(a) $M \approx 0.47$.

Figure 5.- Time history of accelerated turn maneuvers for several representative Mach numbers.

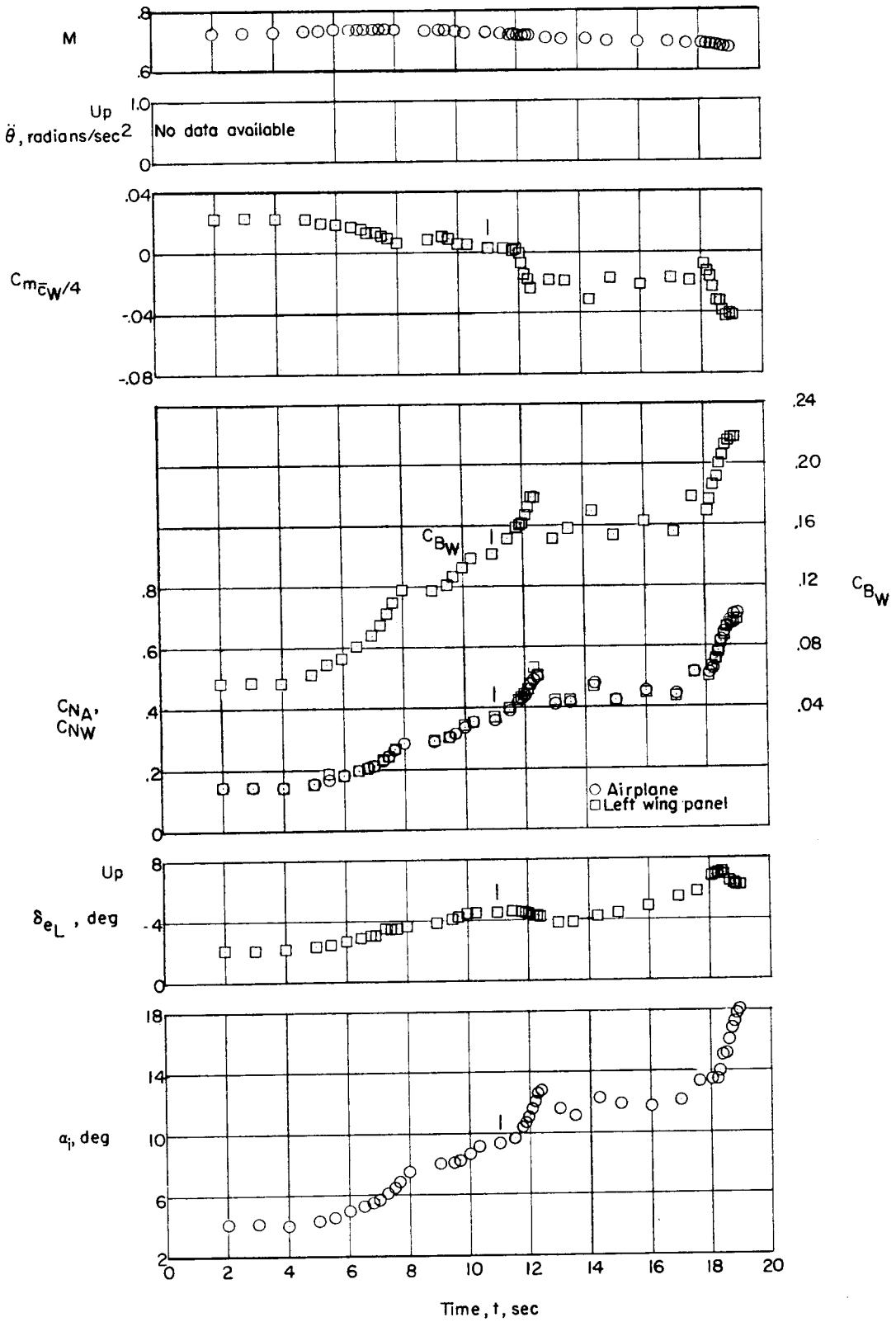

(b) $M \approx 0.73$.

Figure 5.- Continued.

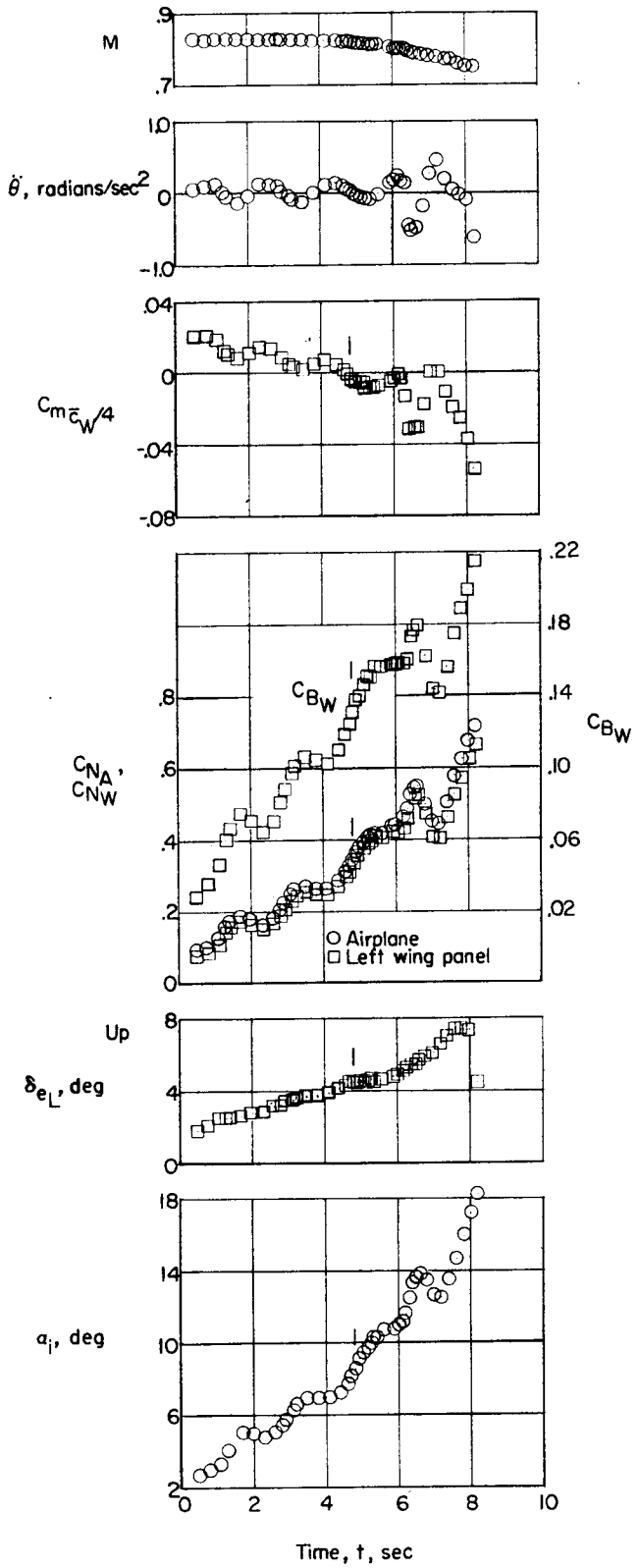

(c) $M \approx 0.83$.

Figure 5.- Continued.

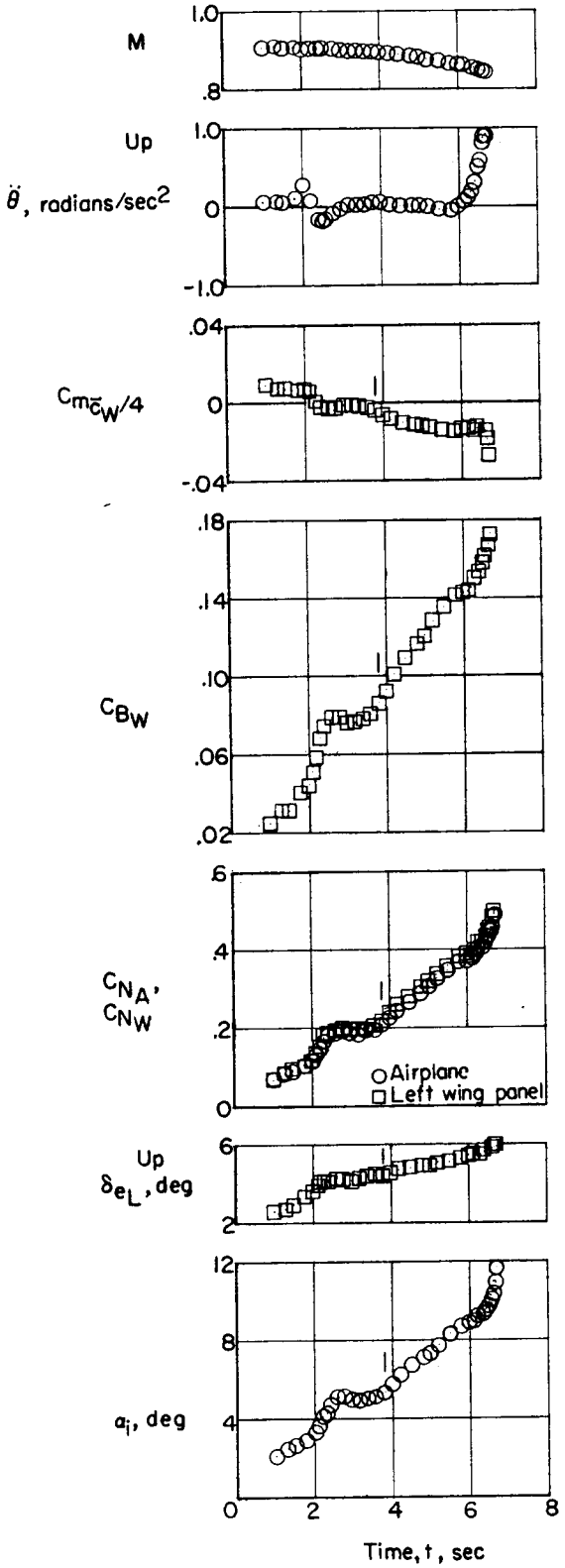

(d) $M \approx 0.91$.

Figure 5.- Continued.

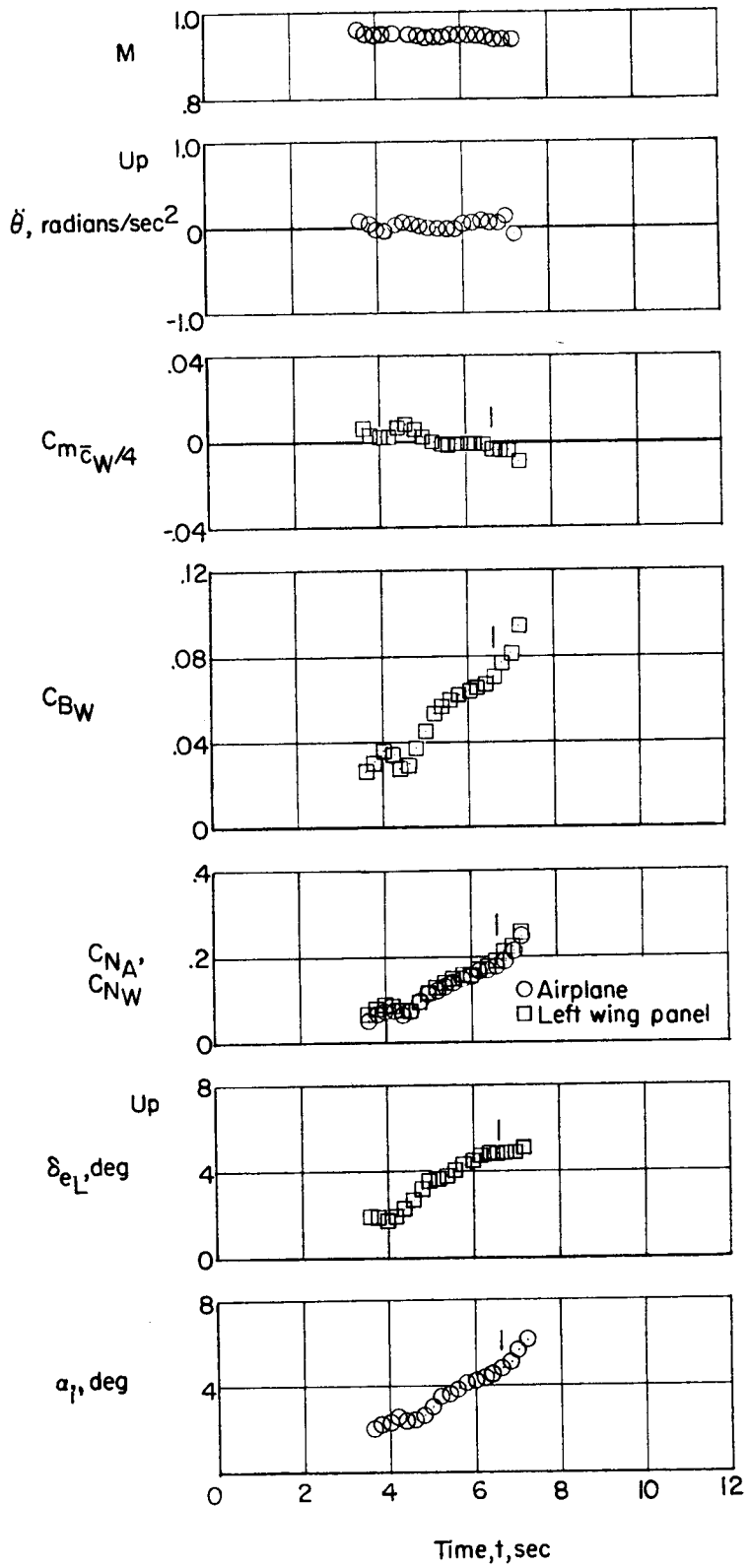

(e) $M \approx 0.95$.

Figure 5.- Concluded.

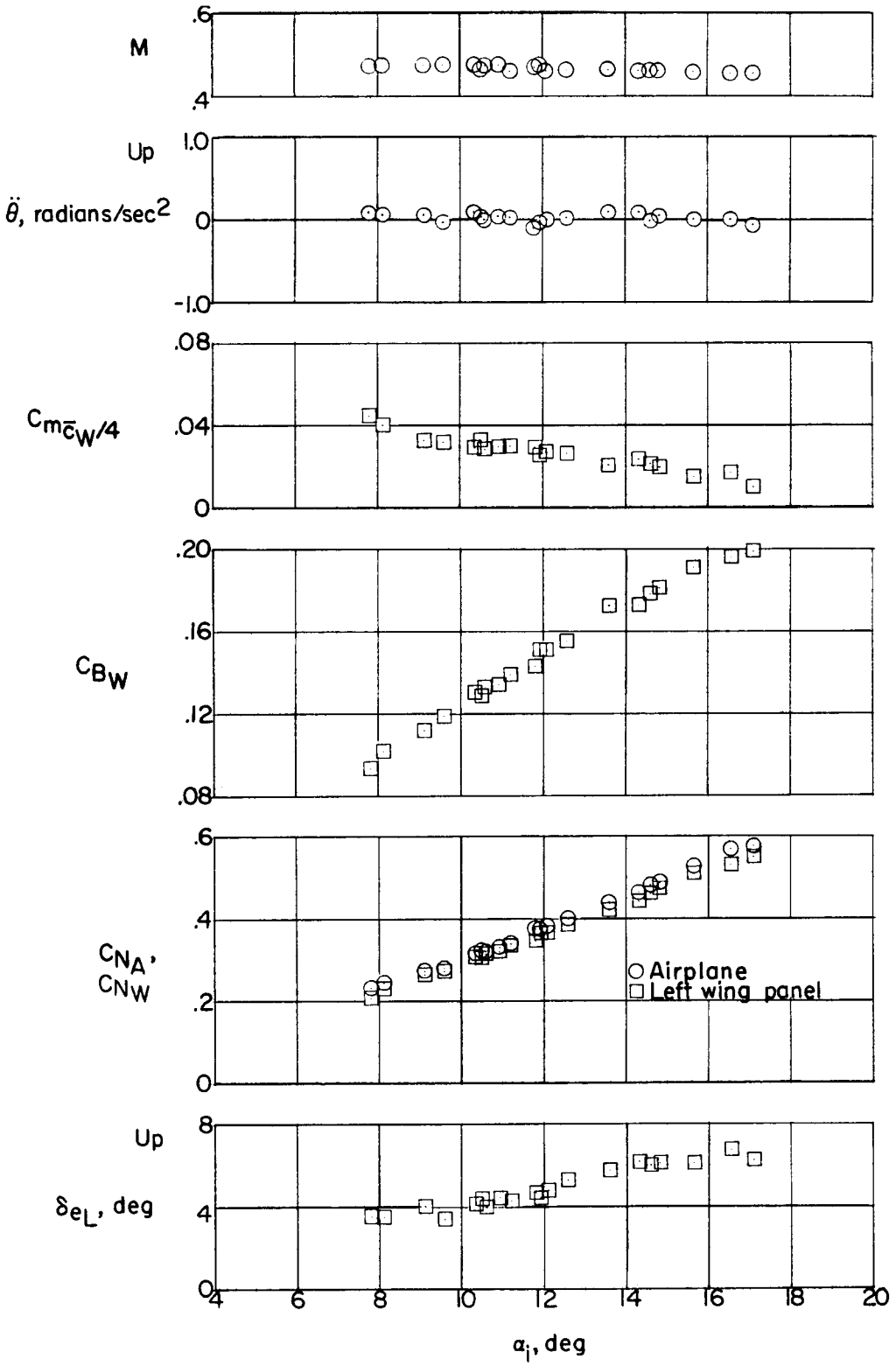

(a) $M \approx 0.47$.

Figure 6.- Variation of measured wing-panel aerodynamic characteristics with indicated angle of attack during accelerated turn maneuvers of several representative Mach numbers.

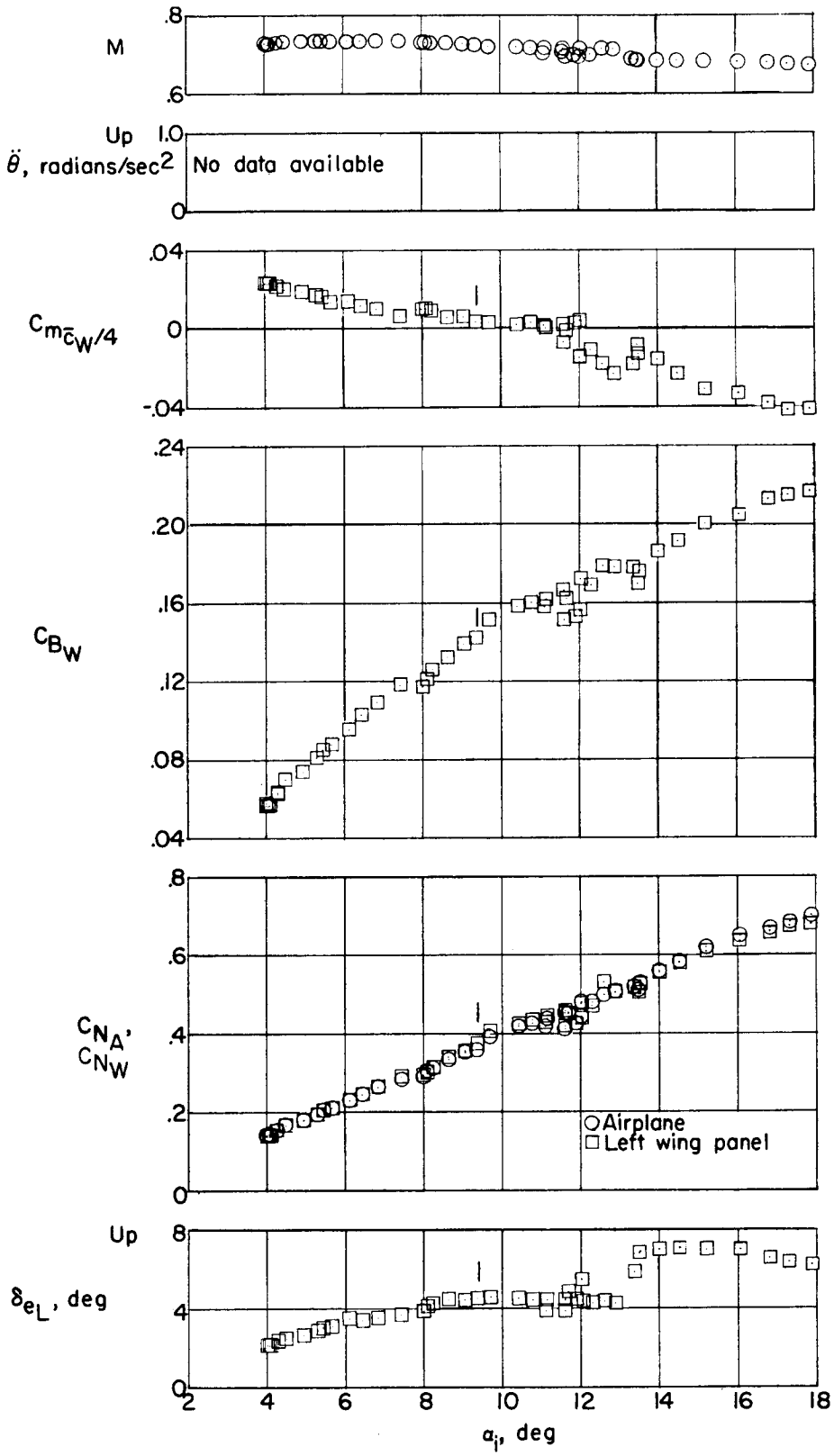

(b) $M \approx 0.73$.

Figure 6.- Continued.

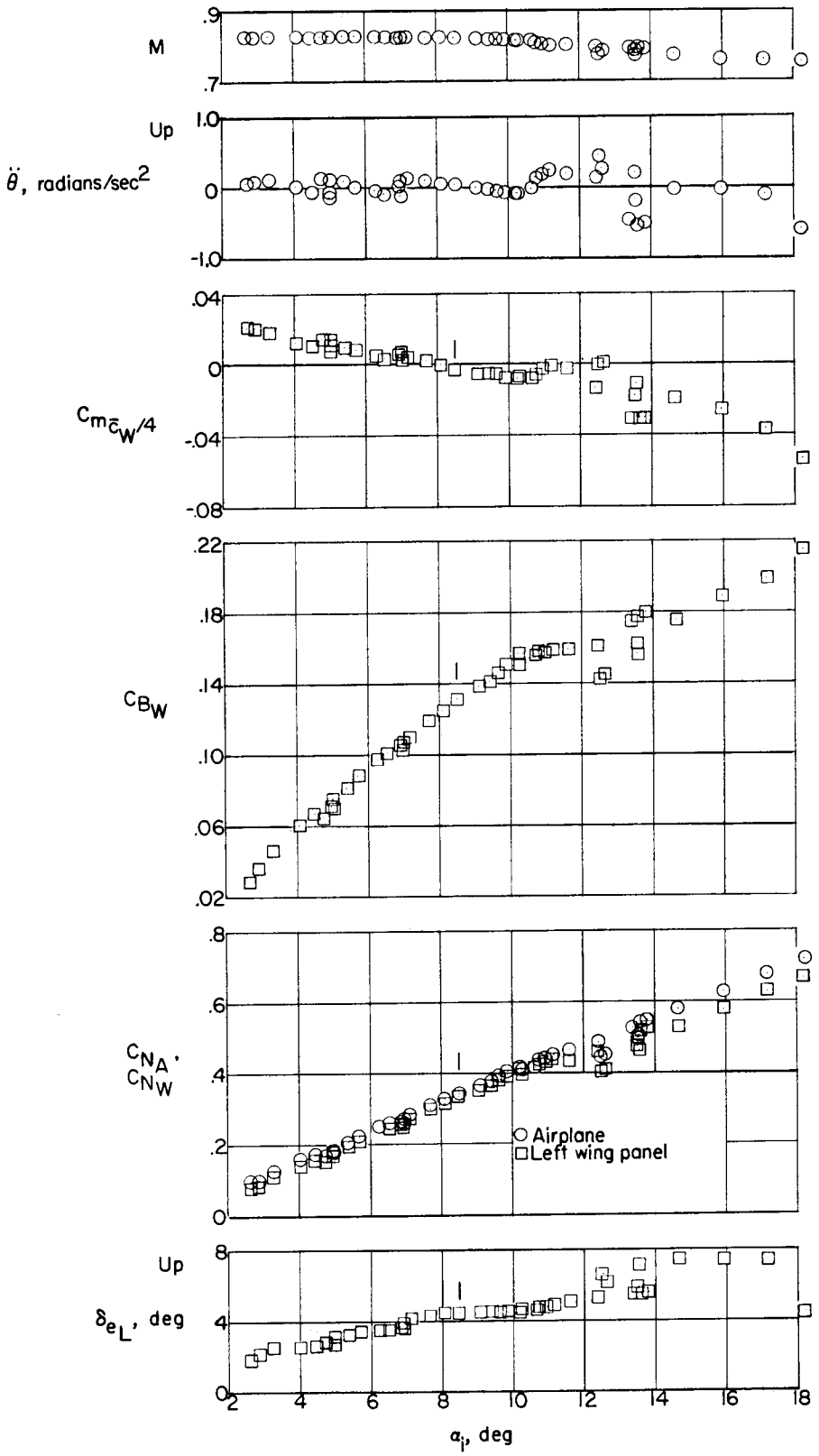

(c) $M \approx 0.83$.

Figure 6.- Continued.

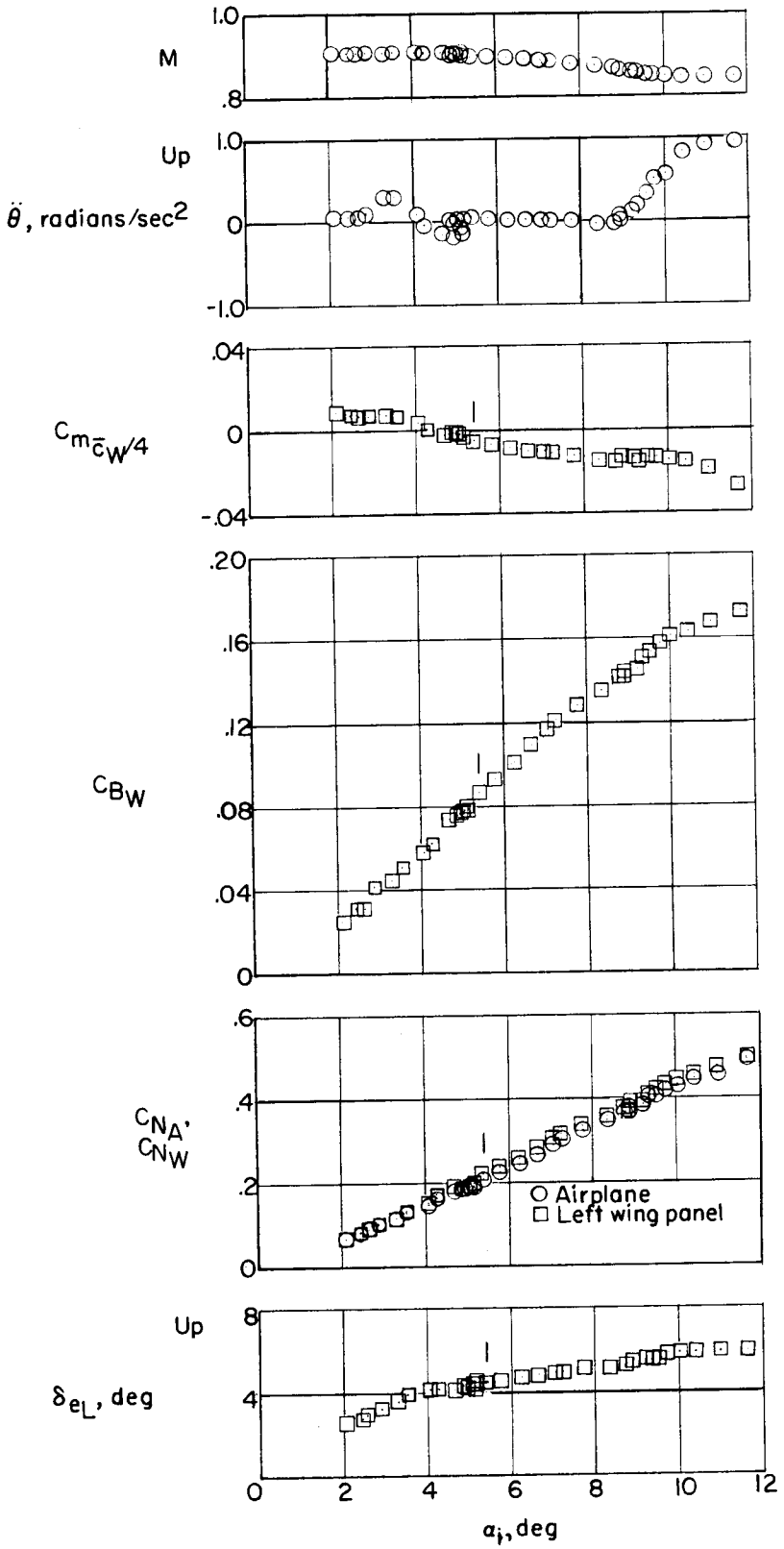

(d) M ≈ 0.91.

Figure 6.- Continued.

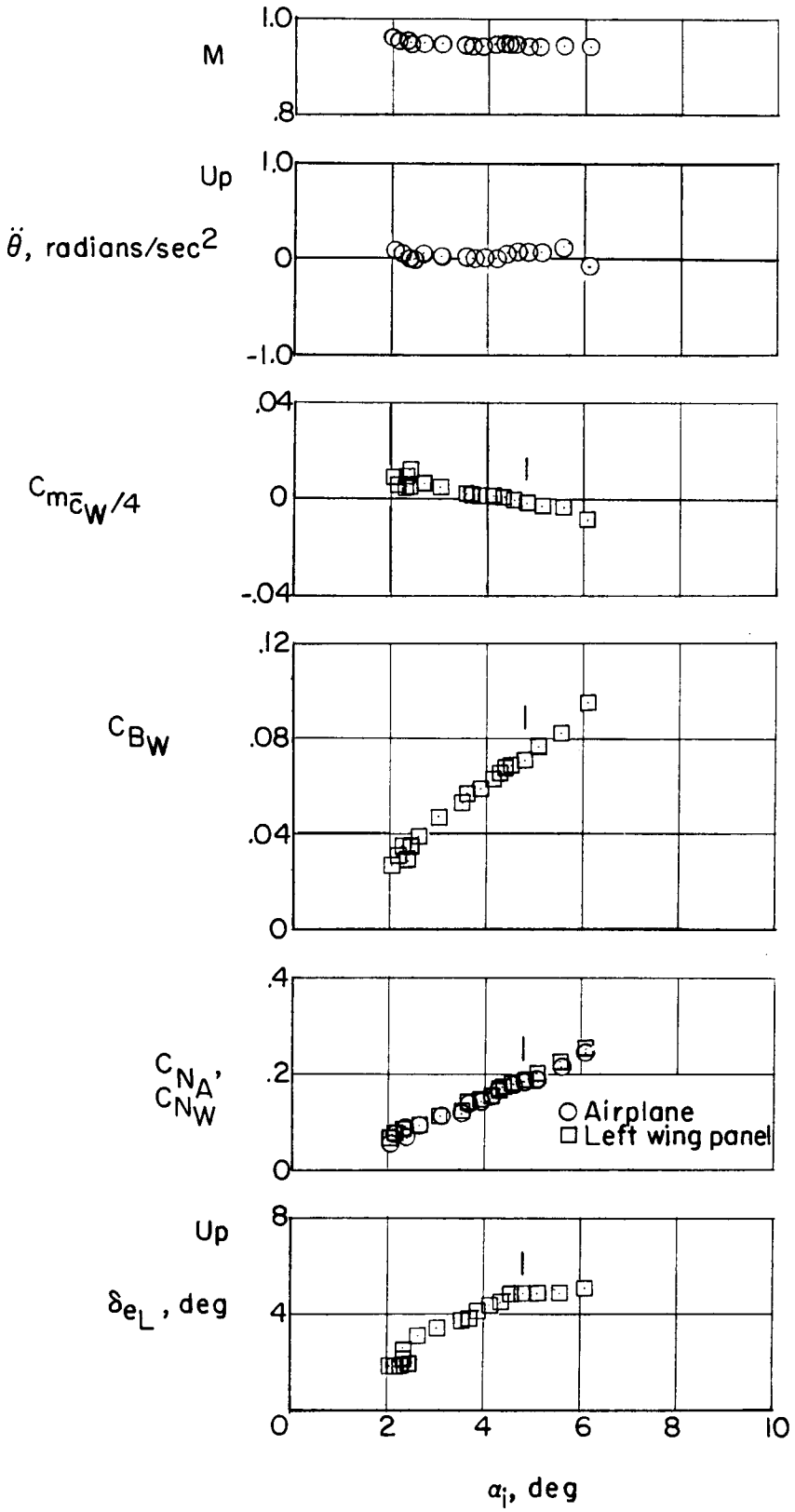

(e) M ≈ 0.95.

Figure 6.- Concluded.

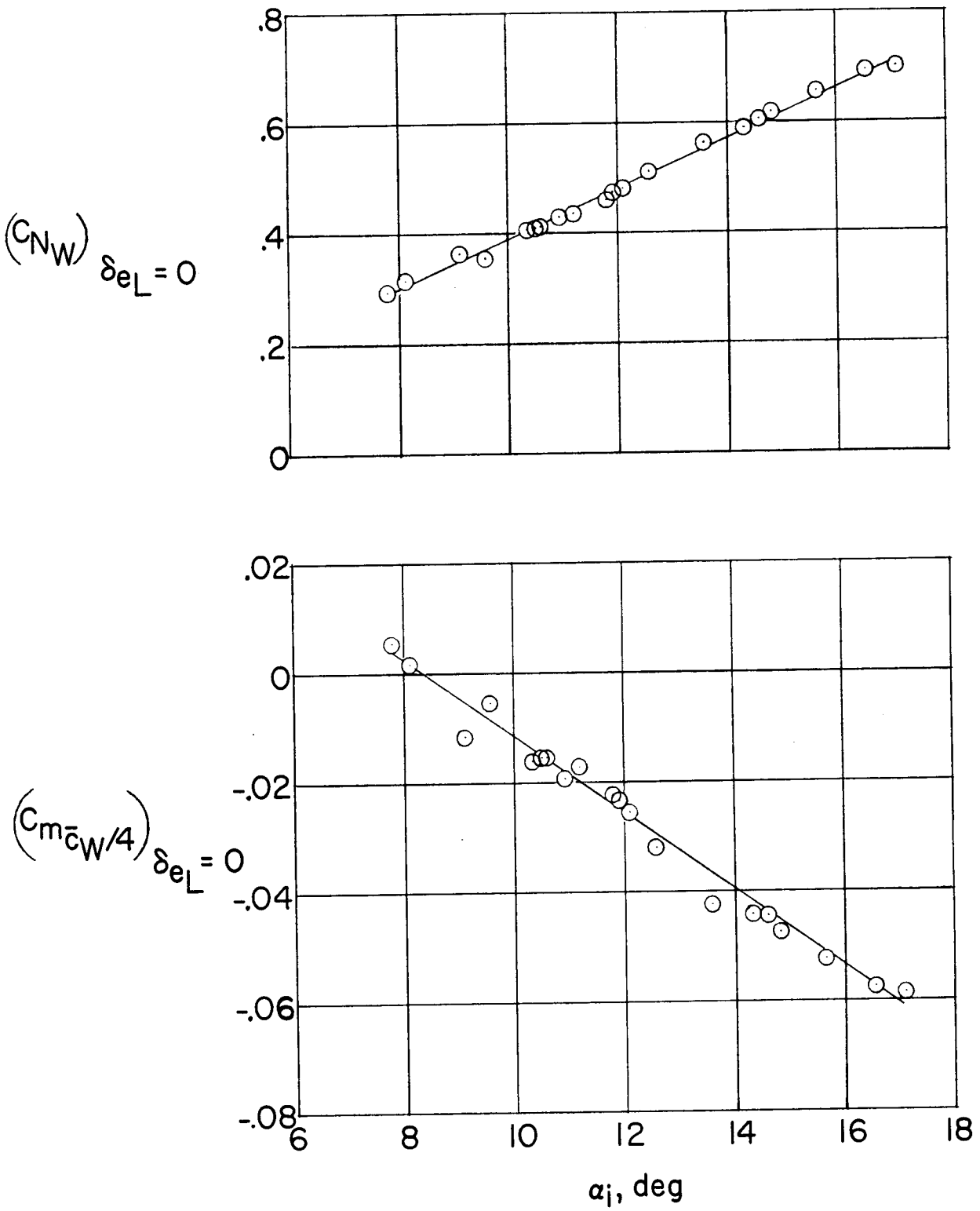

(a) $M \approx 0.47$.

Figure 7.- Variation of wing-panel normal-force and pitching-moment coefficients with angle of attack when corrected to zero elevon deflection.

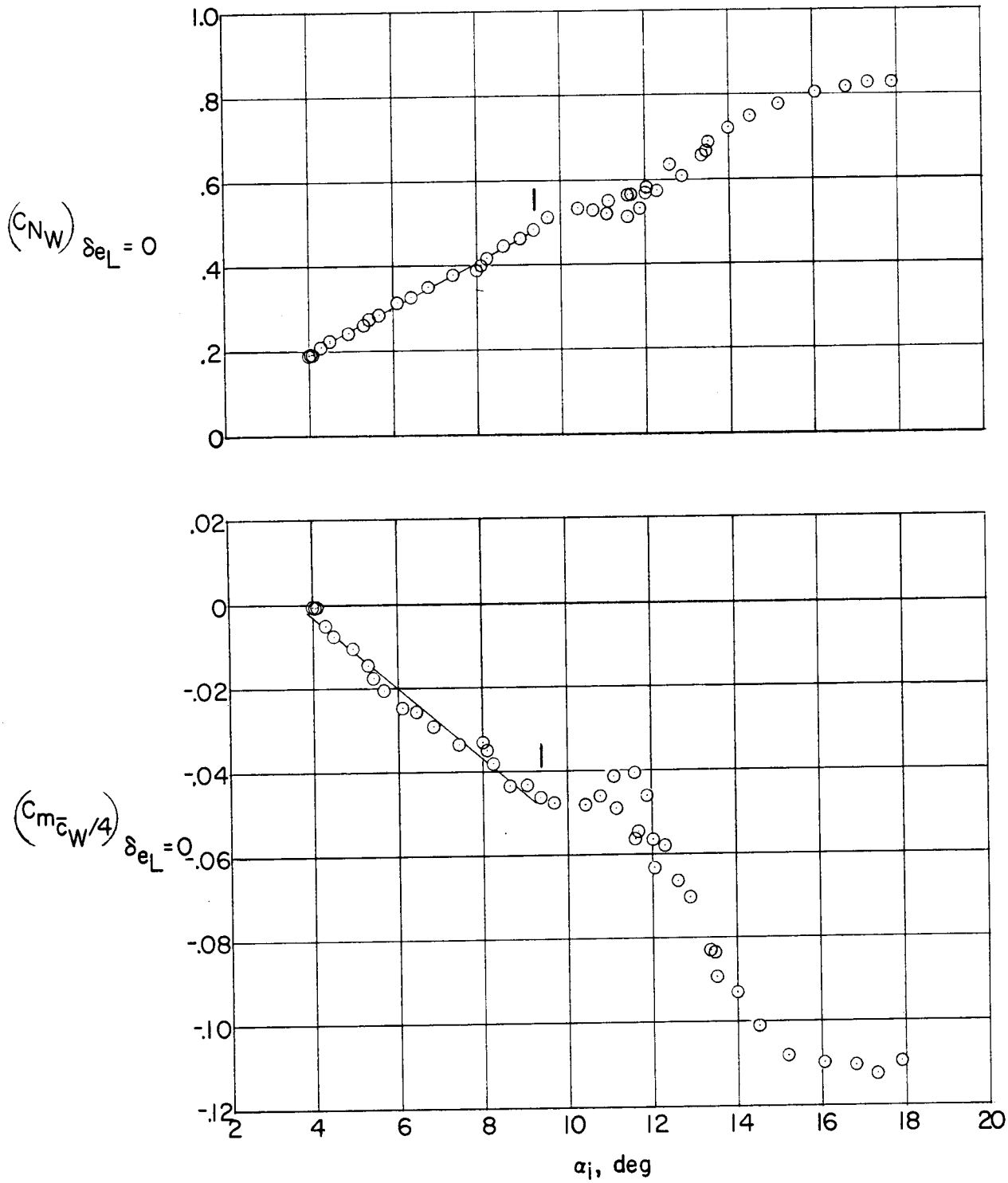

(b) $M \approx 0.73$.

Figure 7.- Continued.

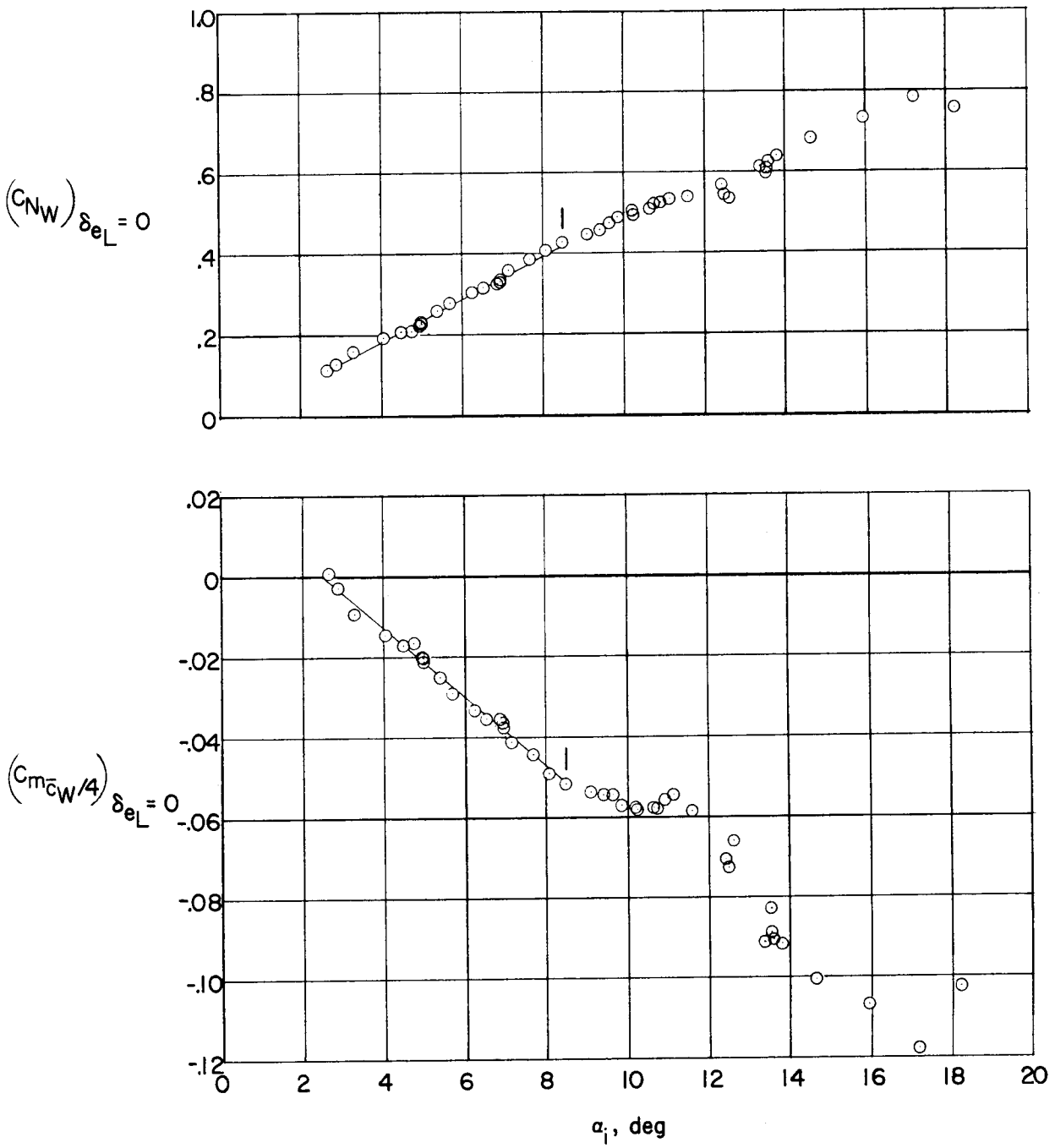

(c) $M \approx 0.83$.

Figure 7.- Continued.

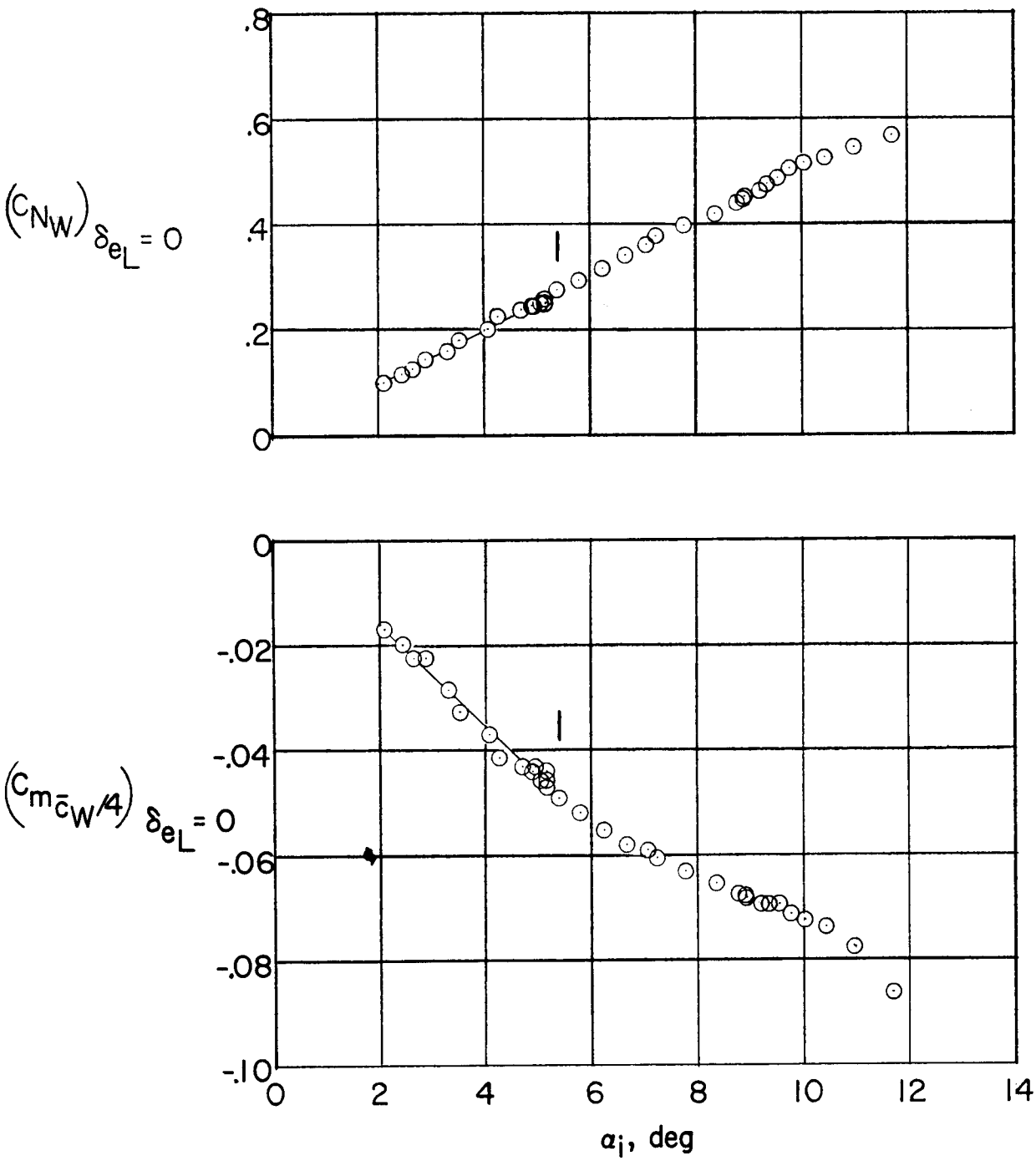

(d) M ≈ 0.91.

Figure 7.- Continued.

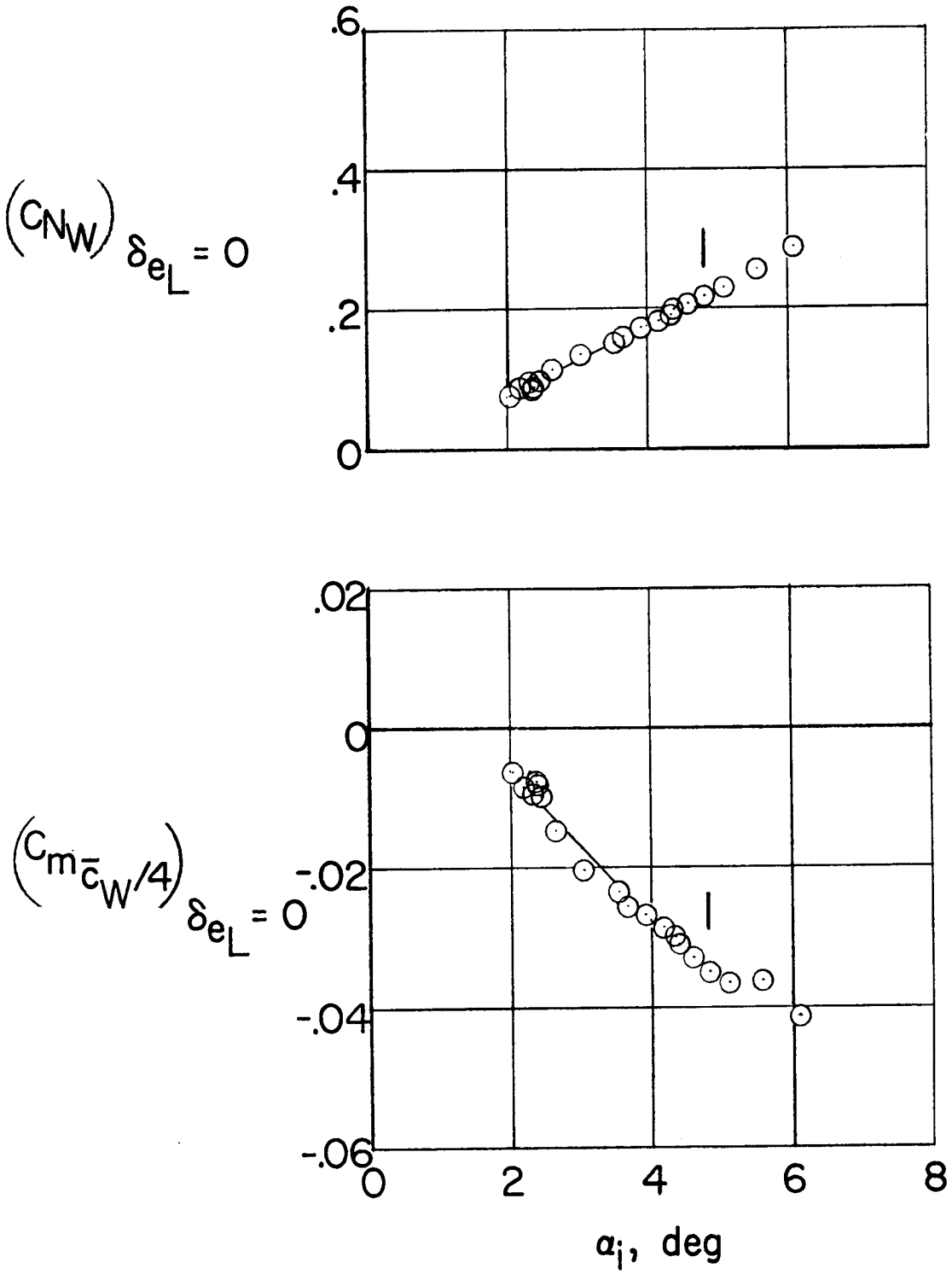

(e) M ≈ 0.95.

Figure 7.- Concluded.

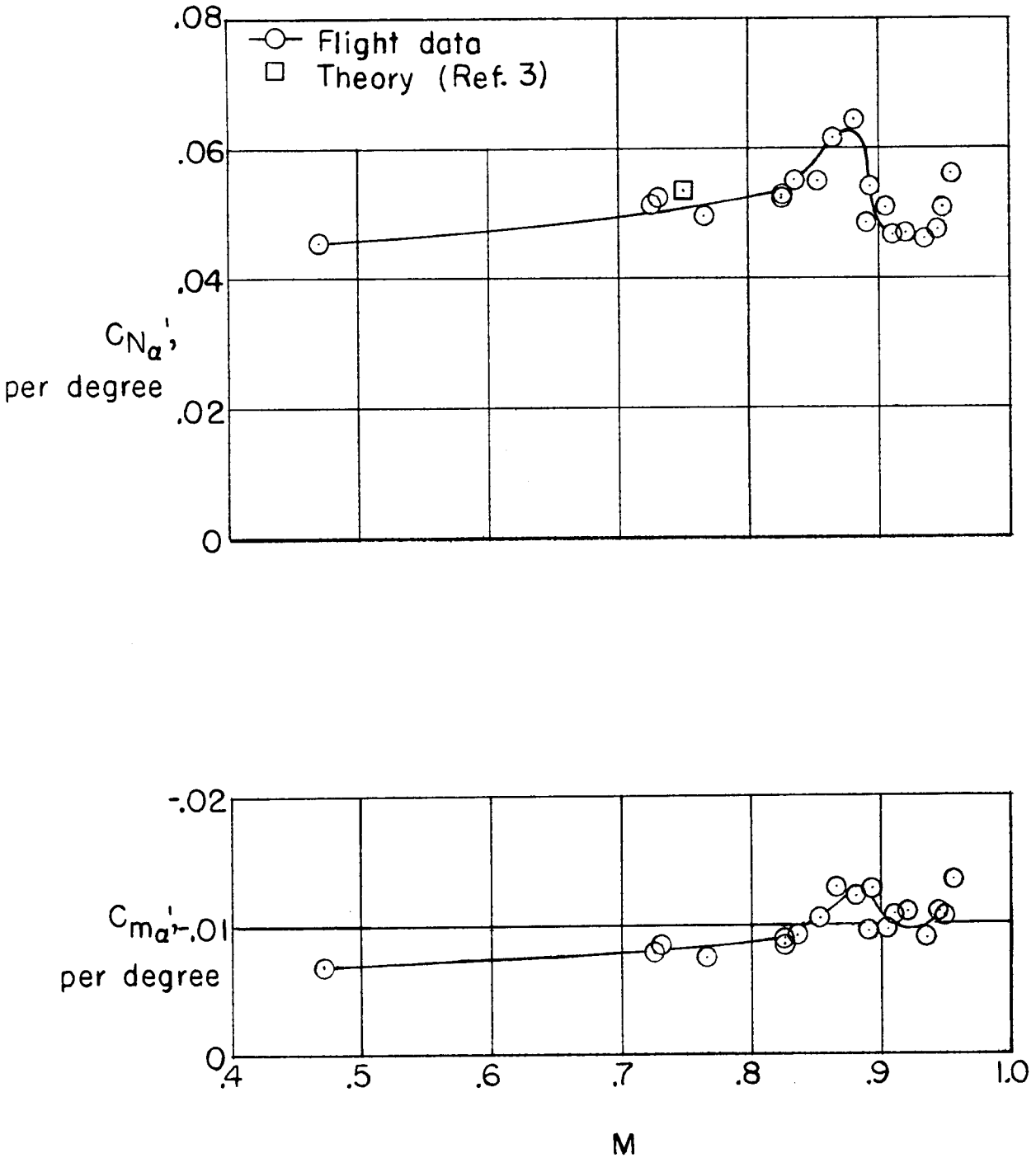

Figure 8.- Variation of wing-panel normal-force curve slope, and static stability parameter, with Mach number, determined from the angle-of-attack region below the point of decreased longitudinal stability.

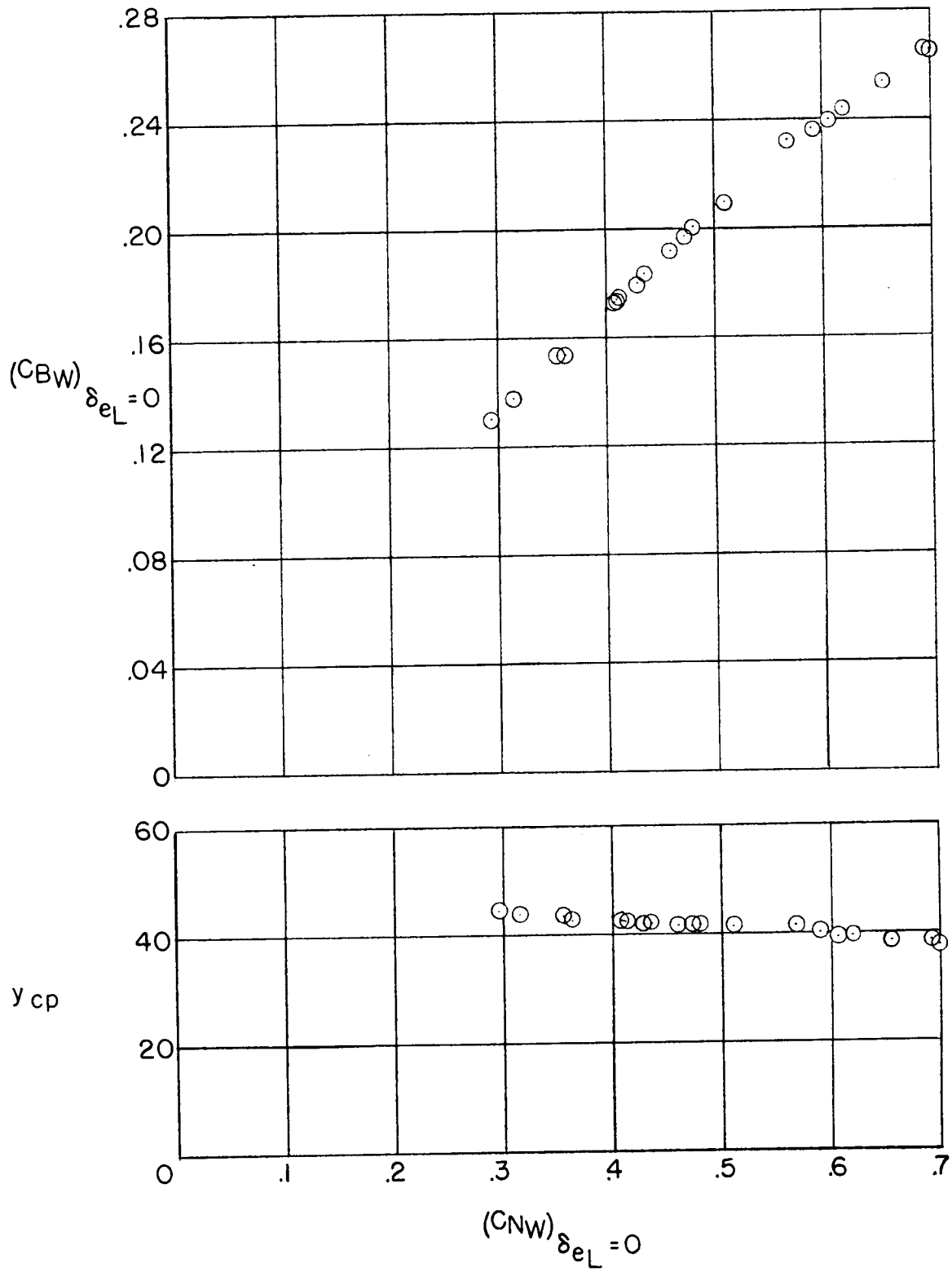

(a) $M \approx 0.47$.

Figure 9.- Variation of wing-panel bending-moment coefficient and lateral center of pressure with normal-force coefficient corrected for zero elevon deflection.

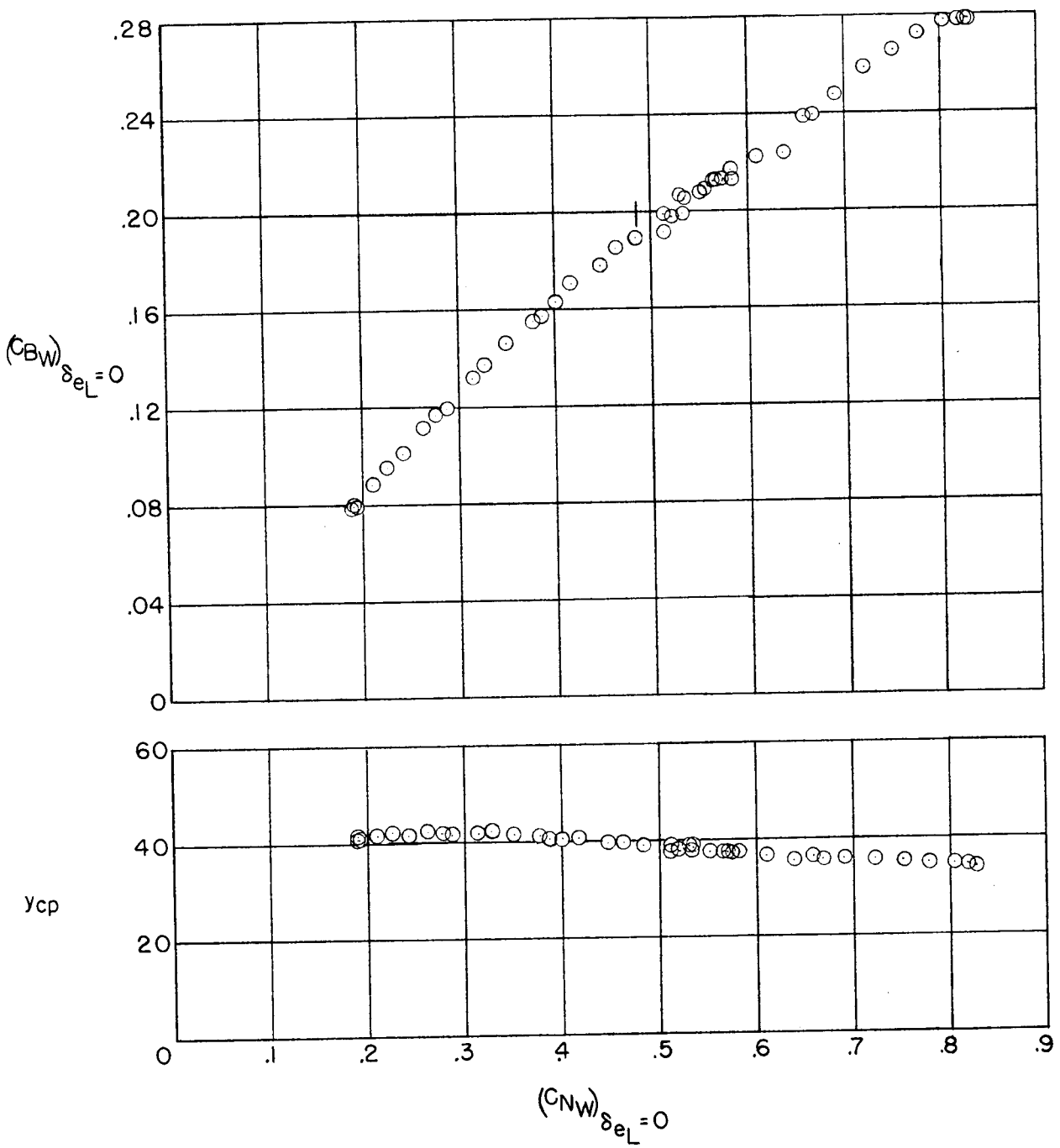

(b) M ≈ 0.73.

Figure 9.- Continued.

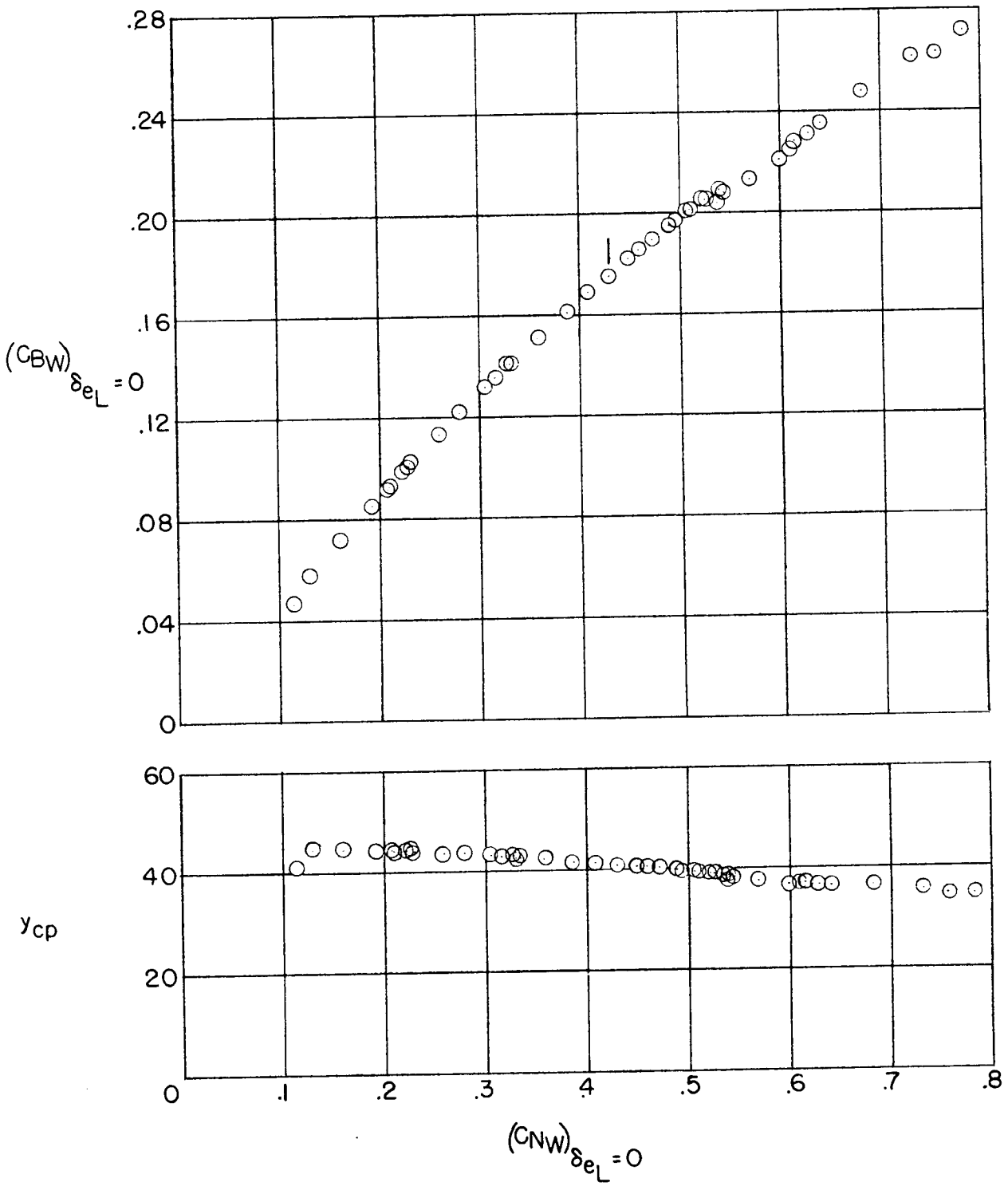

(c) M ≈ 0.83.

Figure 9.- Continued.